

3

## 4 Modeling *E. coli* fate and transport in and around a cattle pond

5

6 Alexander Yakirevich<sup>1,5</sup>, Alisa Coffin<sup>2</sup>, James Wilmer<sup>3</sup>, Oliva Pisani<sup>2</sup>, Robert Hill<sup>1</sup>, Yakov Pachepsky<sup>4</sup>

7 <sup>1</sup>Department of Environmental Science and Technology, University of Maryland, College Park, MD, 21742, USA

8 <sup>2</sup>USDA-ARS, Southeast Watershed Research Laboratory, Tifton, GA. 31793, USA

9 <sup>3</sup>Department of Food Science AND Technology, University of Georgia, Athens, 30602, GA, USA

10 <sup>4</sup>USDA-ARS Environmental Microbial and Food Safety Laboratory, Beltsville, MD, 20705, USA

11 <sup>5</sup>Zuckerberg Institute for Water Research, J. Blaustein Institutes for Desert Research, Ben Gurion University of the Negev,  
12 Sede Boker Campus, 8499000, Israel

13 Correspondence to: Yakov Pachepsky ([yakov.pachepsky@usda.gov](mailto:yakov.pachepsky@usda.gov))

14 **Abstract** Contamination of surface water is a concern for public health. Lands used for animal production are sources of fecal  
15 microorganisms that can reach water bodies, impact their quality, and adversely affect their potential uses. Understanding the  
16 mechanisms of microbial transport through surface/subsurface flow is imperative to predict surface water contamination and  
17 to assign management strategies for enhanced water quality. The aim of this work was to develop and test a mechanistic  
18 numerical model to simulate watershed-scale surface/subsurface water flow, bacteria release from cow manure, and their fate,  
19 as well as transport to a cattle pond. The integrated surface-subsurface hydrological platform HydroGeoSphere (HGS) was the  
20 basis for the site-specific model. The pond and its environs were monitored for 15 months for *Escherichia coli* (*E. coli*)  
21 concentrations, which remained relatively high throughout the study. The model was applied to simulate *E. coli* bacteria  
22 transport in a grassed drainage basin grazed by a permanent herd of approximately 50 cattle. Most model parameter values  
23 were adopted from the literature. The model explicitly accounted for cow excretion to the pond as a source of microbial  
24 contamination. The latter was estimated from the time spent by cows in the pond, which in turn was estimated from imagery  
25 obtained with eight trail cameras installed to cover the pond surface. Images were obtained every 15 min. Simulations for two  
26 years showed that the non-calibrated model replicated spatiotemporal patterns and peak *E. coli* concentration reasonably well.  
27 The *E. coli* cumulative flux loaded by cattle excretion directly to the pond was around two orders of magnitude greater than  
28 that with the surface flow. The results demonstrate that mechanistic watershed-scale modeling combined with observational  
29 data on cattle behavior can provide useful predictions of microbial contamination in cattle ponds using only readily available  
30 data..

31

### 32 1. Introduction

33 Lands used for animal production, such as cow pastures, are sources of fecal microorganisms that can reach water  
34 bodies, impact their quality, and adversely affect their potential uses. Water runoff during and after rainfall events is an  
35 essential factor causing microbial transport from animal waste on pastures to water sources used for irrigation and recreation.  
36 Public health concerns the fate and transport of pathogenic microorganisms and organisms used as indicators of microbial  
37 pollution, such as *Escherichia coli* (*E. coli*).

38 Mechanistic mathematical modeling has provided essential tools for predicting surface water quality and assessing various  
39 sources causing environmental contamination. Models represented by a compartmental setup use the mass balance, empirical,  
40 and semi-empirical equations (Bradford et al., 2013; Cho et al., 2016; De Brauwere et al., 2014; van der Meulen et al., 2024).  
41 The mechanistic models are based on the mathematical description of the momentum and mass balance equations. They  
42 account for the physicochemical and biological processes via constitutive relations or sub-models and various sources and  
43 sinks internally or through boundary conditions. One of the most popular models of this type is the Soil and Water Assessment  
44 Tool (SWAT), which has often been used to simulate the fate and transport of *E. coli* in streams (Sowah et al., 2020; Kondo  
45 et al., 2021; Iqbal et al., 2019). Both point and non-point microbial pollution have been simulated. For example, Kuang et al.  
46 (2024) used the SWAT model to evaluate *E. coli* concentrations in surface water from domestic sewage and manure in China's  
47 Three Gorges Reservoir region. Such models often simulate fecal contamination in rivers, estuaries, and coastal areas (Gao et  
48 al. 2015; Wolska et al. 2022). Microbial transport has commonly been approximated as a one-dimensional process. Much less  
49 work has been done to simulate 3D flow and transport in environmental settings. Curre et al. (2024) gave an example and  
50 developed a model for simulating reactive microbial transport in river-groundwater systems. The model was implemented in  
51 the integrated surface-subsurface hydrological platform HydroGeoSphere (HGS) (Therrien et al., 2010). The authors produced  
52 a synthetic example emphasizing reactive microbial transport in riverbank filtration settings, aiming to quantify microbial  
53 water quality in the aquifer with the pumping wells, which is crucial to improve drinking water management. The HGS  
54 software can be applied to various water bodies, including ponds.

55 Ponds are important sources of agricultural water in rural environments. From 2.6 to 9 million ponds are used for irrigation,  
56 recreation providing water to the livestock, and habitats for wildlife in the United States (Renwick et al., 2006). Little attention  
57 has been paid to modeling microbial water quality in agricultural ponds. Vazquez et al. (2021) developed a mechanistic,  
58 runoff-driven bacterial transport model to simulate peak bacterial concentration events for two highly variable irrigation ponds  
59 in West Central Florida. The authors assumed that surface runoff driven by rainfall events is the primary mechanism driving  
60 microbial contamination in these ponds. The calibrated model predicted *E. coli* peak events relatively well, but did not consider  
61 the spatial distribution of pathogens in and around the ponds. Stocker et al. (2020) utilized the EFDC software to simulate the  
62 fate and transport of *E. coli* in irrigation pond during the water extraction. These authors did not account for sources of  
63 microbial contamination around the pond.

64 The Georgia Coastal plain, USA, has more than 13,000 farm ponds with typical surface area from one to four hectares  
65 (Yao et al., 2024). Many of them are used as cattle ponds, given that the average high summer temperature is around 32 °C. It  
66 is common for agricultural producers to impound water by constructing earthen dams across small streams, thereby capturing  
67 and storing surface water. Additional water is often pumped from deeper aquifers to supplement the water supply (Albright et  
68 al., accepted). These ponds tend to be relatively small (~2 ha) and shallow (< 3 m) and may be used for more than one purpose,  
69 including irrigation, recreation, aquaculture, and a source of water for livestock, or "cattle ponds." Cattle ponds are farm ponds  
70 used by cattle and other livestock animals, providing a perennial supply of available water for drinking and cooling on hot  
71 days. Animals stocked in pastures are typically given free access to cattle ponds within the enclosed areas to wander and stay

72 at will. An essential feature of cattle ponds is the direct input of organic matter and enteric microorganisms into the aquatic  
73 system when the animals eliminate waste. The microbiological quality of water is an essential issue because these waterbodies  
74 are used as a source of drinking water for animals and crop irrigation. This raises concerns regarding microbial contamination  
75 of water that may be used for consumption, either by animals or as irrigation inputs. However, to our knowledge, the microbial  
76 quality of water in cattle ponds and the factors that influence it are poorly understood.

77 The farmers typically lack the resources to monitor their ponds. That limits opportunities for model calibration. Therefore,  
78 it may be beneficial to apply modeling and to determine the accuracy of simulating the microbial quality of water that can be  
79 achieved without model calibration.

80 The overarching objective of this work was to advance the current understanding of microbial contamination in cattle  
81 ponds by integrating watershed-scale hydrological modelling, field monitoring of *E. coli* concentrations, and observational  
82 quantification of cattle presence in the pond. We aimed to develop a modelling framework that would explicitly represent  
83 both hydrologic transport pathways and direct microbial loading by livestock, providing new insight into the dominant  
84 mechanisms controlling microbial water quality in agricultural ponds. The specific objectives of this work were to (a) carry  
85 out spatiotemporal monitoring of the *E. coli* concentrations in a typical farm pond in Georgia where cattle grazed on the  
86 surrounding land had uninterrupted access to water to drink and cool off; (b) monitor and quantify the presence of cattle in the  
87 pond, and (c) develop an *E. coli* fate and transport hydrologic model that would include transport of manure borne *E. coli* to  
88 the pond, direct deposition of animal waste to the pond, and mixing within the pond.

89

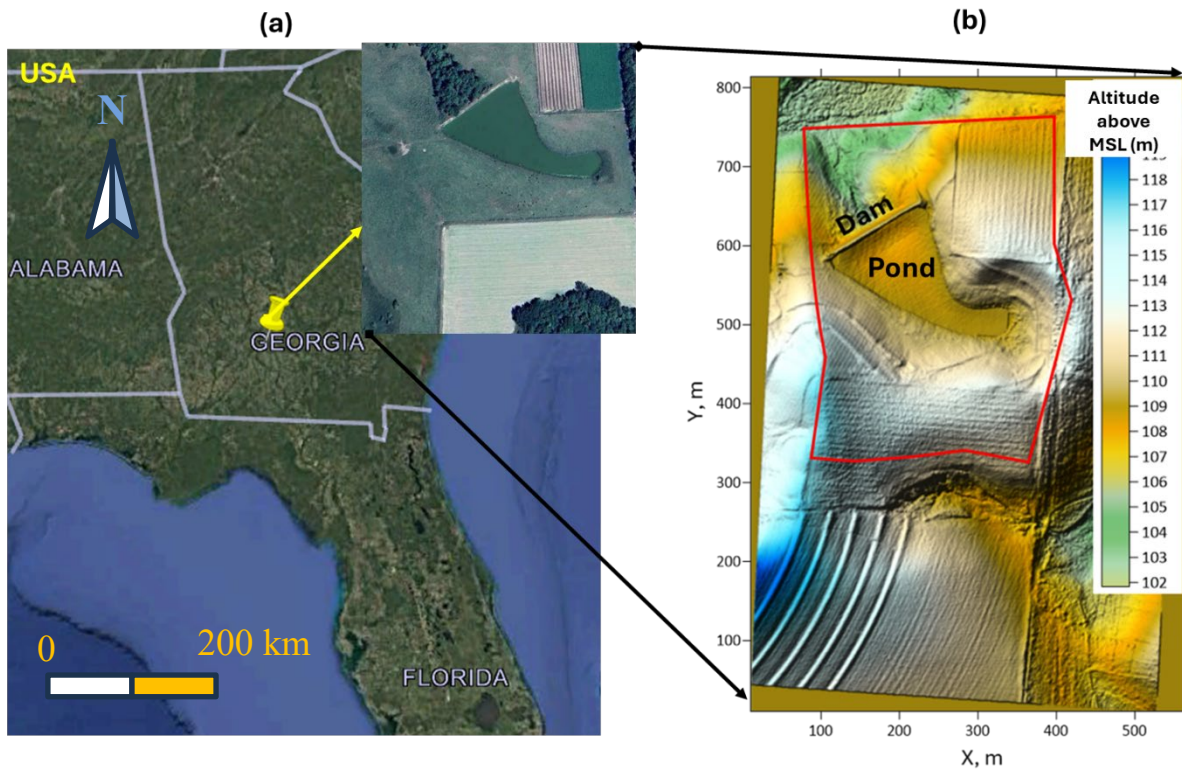
## 90 **2. Materials and Methods**

### 91 **2.1. Study area and environment**

92 The study area is a small watershed (area ~0.45 km<sup>2</sup>) with a pond within a larger, fenced pasture, located on a privately owned  
93 crop-livestock integrated farm in the southern Coastal Plain of Georgia, USA (Figure 1a). The farm is referred to as the Sumner  
94 Cooperator Farm (SCF). Currently, the area is used for cow grazing. The climate is humid subtropical, with a mean annual  
95 temperature of 18.8 °C and mean annual precipitation of 1174 mm.

96 The land surface's Digital Elevation Model of 1 m resolution was downloaded from the Open Topography portal  
97 (<https://portal.opentopography.org/>). The altitude of the land surface varies from 101.8 to 119.7 m (Figure 1b).

98



99

100

101 **Figure 1. Location from Google Earth© Google Earth) images (a) and land topography of the study area (b). The red line represents**  
 102 **the boundary of the simulation domain,**

103

104 Soil cover at the site consists of a loamy sand (average of 85% sand, 9% silt, and 7% clay) to depths of 60-80 cm,  
 105 underlain by sandy clay loam (average of 62% sand, 8% silt, and 30% clay) containing plinthite, a low permeability layer of  
 106 hard iron-rich soil restricting hydraulic connectivity between surface and groundwater (Blume et al., 1987). The latter soil was  
 107 used to build the bottom of the pond and the dam.

108

109 Weather conditions were monitored by the USDA-ARS Southeast Watershed Research Laboratory (SEWRL) at the  
 110 site to measure air temperature and humidity, wind speed, solar radiation, and soil and water temperature. Data were collected  
 111 from a climate station located at the SCF noted as "Rain Gage 80" in the SEWRL public data website  
 112 (<https://radio.tiftonars.org/rg80.htm> ). Specifications for instrumentation follow the configurations for the Little River  
 Experimental Watershed climate stations described in Bosch et al. (2007).

## 113 2.2 Quantifying pond use and bacterial concentrations in cattle manure

114

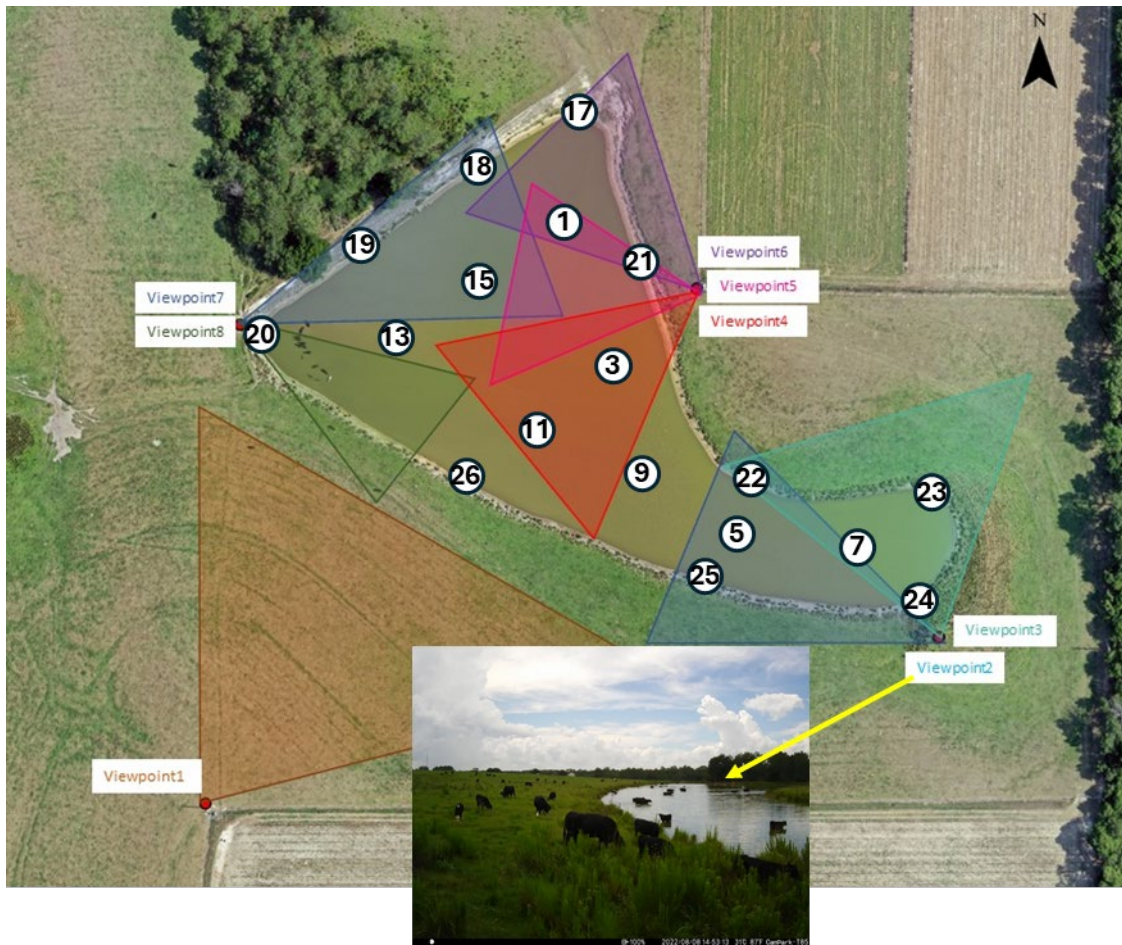
115 Cattle use of the pond and the pasture area draining into the pond was evaluated using automated trail cameras. Eight cameras  
116 were fixed to solid structures (e.g., fence posts, trees) and their fields of view (FOVs) captured overlapping images of the pond  
117 at regular intervals. Three comparable camera models were used for the study, including 3 Bushnell 24MP Prime Low Glow  
118 (Model 119932C), 3 CamPark, and 2 Coleman (Model CHD400W) cameras. Cattle in the pond were imaged from July 2022  
119 to December 2023. Secure digital (SD) removable media cards were used to record the imagery and were replaced every 6 to  
120 10 weeks for the duration of the study. Imagery was downloaded and stored on a file server for subsequent analysis. The  
121 imagery was visually assessed for pond use by cattle by a single observer for all days. Images were reviewed from each camera,  
122 and the number of cows in the pond was counted in each image. Tallied viewpoint counts were summed according to the model  
123 finite element mesh (FEM) nodes segmentation of the shoreline described below, multiplied by the time interval of the camera  
124 setting (5 to 30 minutes), and divided by 1440 minutes per day. The resulting values were summed for each shoreline segment  
125 to produce a daily value of "cow days" (Cex). To evaluate the accuracy of the visual assessment, two additional independent  
126 observers conducted validation counts of a sample of the imagery following the same protocol, and agreement among the three  
127 observers (OBS1, OBS2, and OBS3) was evaluated (Table S1).

128         Between February and May 2023, 18 fresh cow manure samples were collected from the area around the pond.  
129 Samples were collected into 50-mL conical tubes using a sterilized tongue depressor and were then placed on ice for storage  
130 and transport to the laboratory. Laboratory processing of manure samples occurred within 24 hours of sample collection.  
131 Briefly, 2g of manure was blended with 200 mL of sterile, deionized water for 2 min on the highest setting. Mixed samples  
132 were then allowed to settle for 15 minutes before aliquots were used to prepare serial dilutions of the manure mixture. Diluted  
133 manure solutions were processed in duplicate using the Colilert method (IDEXX, Westbrook, Maine), which produced a most-  
134 probable-number (MPN) of *E. coli* in each sample. An MPN was then calculated per mass of manure (MPN *E. coli* kg<sup>-1</sup>) using  
135 information from a dry weight analysis of the manure.

### 136 **2.3. Water sampling**

137         Figure 2 shows the locations of the water sampling points for measurements of *E. coli* concentration and of the camera  
138 viewpoints for monitoring cattle. For the water sampling points, locations with even numbers (2, 4, 6, 8, 10, 12, 14, 16, not  
139 shown) have coordinates the same as locations with odd numbers (1, 3, 5, 7, 9, 11, 13, and 15), respectively. However, locations  
140 with odd numbers were sampled at the pond surface, whereas locations with even numbers were sampled at a depth of 50 cm  
141 using a peristaltic pump. Locations 17 to 26 were sampled at the surface near the banks. All samples were taken between 10:00  
142 and 12:00 in the absence of cows.

143



144

145

146 **Figure 2. Locations of water sampling points (1-26) and cattle monitoring cameras (Viewpoints 1-8). The insert shows an example**  
 147 **of an image taken at monitoring viewpoint 2. Orthoimage from July 7, 2022 by USDA-ARS, Southeast Watershed Research**  
 148 **Laboratory, Remote Sensing and Mapping Group, Tifton, Georgia, USA. The imagery was collected with a Hasselblad L1d-20C**  
 149 **20mp camera using a DJI Mavic 2 Pro L1P drone, and created using Pix4D Mapper image processing software.**

150

151

## 152 **2.4 Mathematical model**

153 Accounting for the complexity of hydrogeological and hydrochemical processes, we choose the HGS (Therrien et al., 2010)  
 154 as a basis for the model. In HGS, the flow of water is simulated in a fully integrated mode; water derived from rainfall inputs  
 155 is partitioned into components such as overland and stream flow, evaporation, infiltration, recharge, and subsurface discharge  
 156 into surface water features such as lakes, streams, and wetlands in a natural, physics-based fashion. It employs a fully coupled

157 numerical approach, allowing the simultaneous solution of both the surface and variably saturated subsurface flow, solute  
158 transport, and heat transfer.

159 The mathematical model of the watershed flow and transport comprises the following components. The Richards equation  
160 simulates three-dimensional transient subsurface flow in a variably saturated porous medium (PM domain). The van Genuchten  
161 (1980) relations are used to calculate the pressure-saturation relationship and hydraulic conductivity. The two-dimensional  
162 depth-averaged diffusive wave equation describes overland water flow (OVL domain). The subsurface and surface flow  
163 equations are fully coupled. Evapotranspiration affects surface and subsurface flow domains and is modeled as a combination  
164 of transpiration from vegetation and evaporation. Microbial transport is described by 3D and 2D coupled advection-dispersion  
165 equations in the subsurface and surface, respectively. We chose the linear Henry isotherm for simulating *E. coli* sorption. A  
166 first-order decay reaction describes the bacteria's die-off. **The present model does not explicitly simulate soil and manure  
167 erosion, suspended sediment transport, settling, or resuspension. As a result, bacterial transport is represented primarily through  
168 direct runoff and overland flow pathways, without accounting for attachment to or release from suspended or bed sediments.  
169 However, the model accounts for the release of bacteria from cowpats uploaded onto the soil surface.**

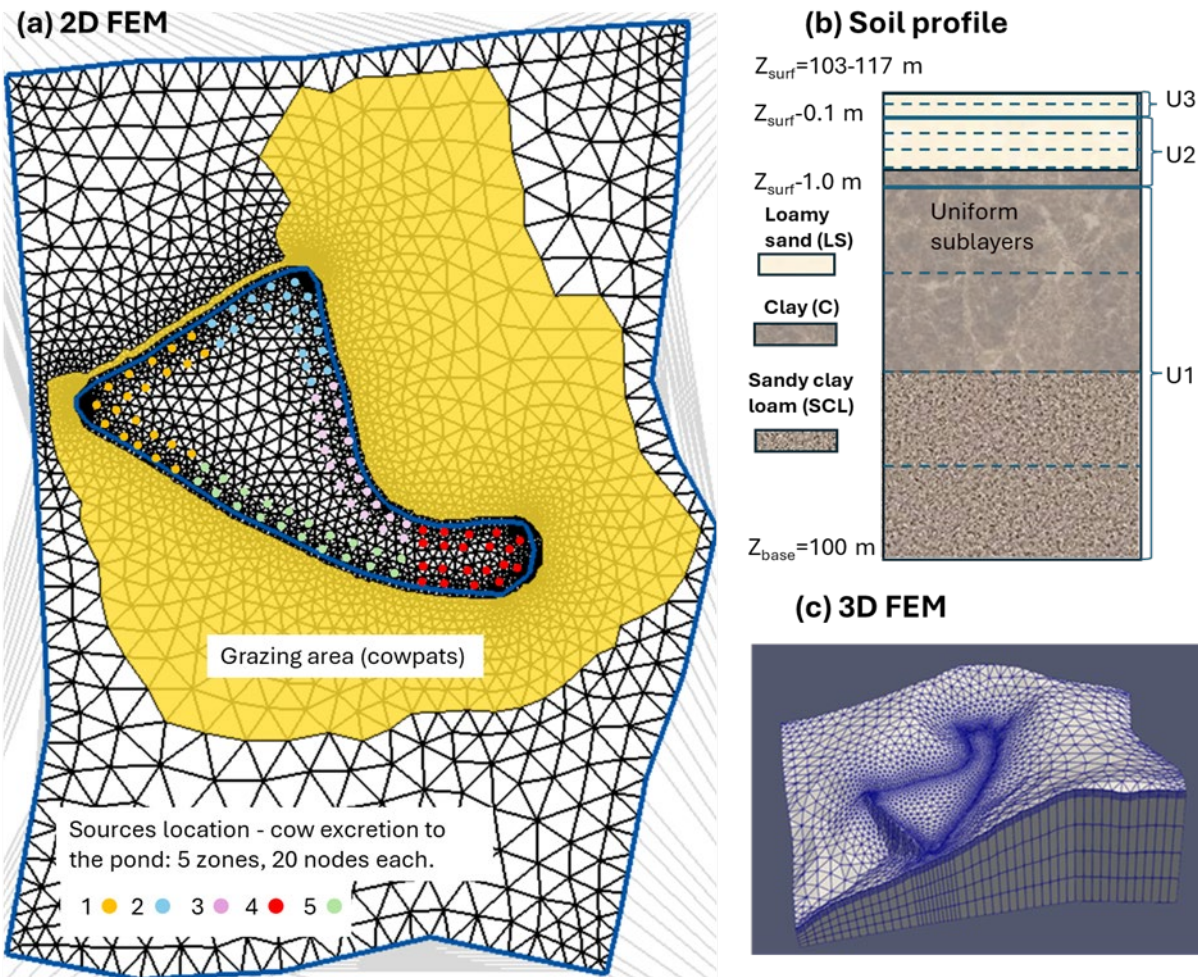
170 The numerical solution of partial differential equations and the initial and boundary conditions are done by the control volume  
171 finite element approach.

172

#### 173 2.4.1. Finite element mesh

174 The numerical setup of the simulation domain is shown in Figure 3. The lateral boundary was chosen to cover most of the area  
175 where runoff water flows towards the pond. The 2D triangular finite element mesh (FEM) was created using AlgoMesh  
176 software ([www.hydroalgorithms.com/software/algomesh](http://www.hydroalgorithms.com/software/algomesh)) (Figure 3a). It consists of 2882 nodes and 5595 triangular  
177 elements. The mesh has the highest density of nodes and elements near the pond boundary.

178 The base of the simulated profile is located at the depth corresponding to an altitude of 100 m. The thickness between the base  
179 and soil surface was divided into three layers (U1-U3, Figure 3b), and each layer was split into 2 to 4 sublayers. The floors of  
180 the layers U2 and U1 are located at depths of 0.1 and 1.0 below the land surface, respectively, thus mimicking the surface  
181 topography. In the model, each sublayer is considered an independent layer defining the height of triangular prisms, which  
182 presents the vertical extension of the 2D plane mesh within each layer (Figure 3c).



183  
 184 **Figure 3. Numerical model setup:** (a) The 2D triangular finite element mesh in the simulation domain. Cowpats (a flat, round piece of cow dung) are  
 185 located in the yellow color area. Colored circles represent the location of sources to simulate cattle excretion in the pond. (b) Schematic representation  
 186 of numerical mesh layers in the simulated profile. Solid and dashed horizontal lines represent the boundaries between layers and sublayers,  
 187 respectively. (c) 3D finite element mesh (FEM).  
 188

189 **2.4.2. Initial conditions**

190 Initial conditions were obtained by running multi-year simulations. For the subsurface flow, a constant head of -2 m in each  
 191 node of the finite element mesh was used. For the surface domain, the initial water depth was  $10^{-7}$  m in each node, i.e., the  
 192 pond was assumed to be empty. These initial conditions were corrected during simulations: 1) For two years, a constant  
 193 precipitation rate (flux at the soil surface of 0.01 m/day) was simulated to "fill in" the pond with water and establish a steady-  
 194 state flow regime in the simulation domain; 2) the resulting distribution of heads was taken as a new initial condition and the

195 model was run with varying precipitation and evapotranspiration for 6 years to establish a quasi-stationary flow regime; 3)  
196 Finally, the initial conditions were taken from the results obtained at the end of the simulations.

197 Initially, the prescribed concentration of bacteria was equal to 0 everywhere in the domain. Then, during multi-year  
198 simulations, a concentration distribution was developed in the simulation domain, exhibiting cyclic behavior with time, and it  
199 was accepted as the initial condition for January 1, 2022.

200

### 201 **2.4.3. Boundary conditions and internal source terms**

202 In the study area, the groundwater level of a regional artesian aquifer was detected at around 70 meters above mean sea level  
203 (mamsl) (Watson, 1976), which is 30 m below the bottom (100 m) of the simulated domain. Therefore, the groundwater is not  
204 included in simulations. The free drainage boundary condition at the bottom and no flux at the lateral boundaries were  
205 prescribed.

206 At the soil surface, time-variable precipitation rate and evapotranspiration were prescribed. The latter is calculated from the  
207 potential evapotranspiration, computed using the Penman-Monteith equation (Monteith, 1981; Danielescu, 2022).

208 The critical depth boundary condition at the watershed boundary was set to the surface flow domain. The rainfall and  
209 evaporation rates are prescribed as volumetric flow fluxes per unit area.

210 For the bacteria transport, zero-gradient and zero-concentration conditions were set in the subsurface domain along the inflow  
211 and outflow lateral boundaries, respectively. The third-type (Cauchy) boundary condition was set at the surface, expressing  
212 the balance between bacteria's advective flux at the soil surface and their advective and dispersive fluxes below. The land  
213 surface is divided into a grazing area with cowpats and the rest (Figure 3a). Cowpats were assumed to be uniformly distributed  
214 over the grazing area. The boundary concentration (and mass flux) equals zero in the area free from cowpats. For the grazing  
215 area, a sub-model was developed to calculate the boundary concentration of bacteria. The sub-model simulates the daily  
216 evolution of concentration depending on the load of cowpats and the initial concentration of bacteria (see Appendix A for the  
217 equations). On each specific day, the fate of bacteria concentration in cowpats that were loaded during that, and every previous  
218 day was calculated using the Q10 model (Martinez et al., 2013). The latter computes the bacteria's die-off/survival rate  
219 depending on weather conditions. The concentrations of released microorganisms are calculated as a function of precipitation  
220 according to Bradford and Schijven's (2002) equations for each cowpat's load, accounting for the remaining mass of bacteria  
221 during the current day. The resulting boundary concentration is assessed as a sum of those concentrations.

222 Cattle excretion to the pond was simulated by introducing the internal source terms in the FEM nodes (Figure 3a). The  
223 nearshore pond area, where bathing cattle were observed, was divided into five zones. Each zone includes twenty FEM nodes.  
224 These nodes do not coincide with the water sampling locations. The source rates were calculated from the number of cattle  
225 and the time they spent in the pond (Section 3.1). The time-variable boundary conditions and source/sink terms were prescribed  
226 on a daily scale.

227

228 **2.5. Model parameters**

229 We adopted the values of model parameters from different sources or estimated based on existing experimental data or during  
 230 simulations. Tables 1 and 2 present parameter values used in the simulations.

231 **Table 1. The model parameter values for the subsurface domain.**

Parameter	Soil			Source
	Loamy sand	Sandy clay loam	Clay	
Hydraulic conductivity $K_s$ , m d <sup>-1</sup>	1.2(1.28)	0.35(0.36)	0.0001-0.01	Using Rosetta & PSD <sup>1</sup>
Porosity $q_s$	0.39(0.36)	0.45	0.48 (0.46)	Using Rosetta & PSD
Residual water content $q_r$	0.049(0.046)	0.08	0.067(0.098)	Using Rosetta & PSD
van Genuchten $\alpha$ , m <sup>-1</sup>	3.12(3.6)	2.35(2.29)	2.0 (1.5)	Using Rosetta & PSD
van Genuchten $\beta$	1.48(2.02)	1.36(1.35)	1.41(1.25)	Using Rosetta & PSD
Longitudinal dispersivity $a_L$ , m	12.5			Assessed by trial-and-error
Transverse dispersivity $a_T$ , m	2.5			Assigned $a_T=0.2 a_L$
<i>E. coli</i> distribution coeff. $k_D$ , L kg <sup>-1</sup>	14.5			Mankin et al. (2007)
<i>E. coli</i> die-off rate, $k_{s,m,2}(20)$ , d <sup>-1</sup>	0.042(cowpats), 0.111(soil)			Martinez et.al. (2013)
Parameter $Q_{10,m}$	1.48(cowpats), 1.65(soil),			Park et. al. (2016)

232 PSD – particle size distribution

233 |

234 The geology of the subsurface is not well known. The following composition of soil layers was accepted, based on available  
 235 information: loamy sand to a depth of 0.5 m, below which a clay layer of variable thickness extends down to the upper half of  
 236 layer U1 (Figure 3b). The lower half of U1 is presented by sandy clay loam. The pond bottom (to 0.5 m depth) and the dam  
 237 are built from clay with the hydraulic conductivity of 0.0002 m/day.

238  
 239 **Table 2. The model parameter values for the surface and evapotranspiration domains.**

Parameter	Value	Source
Manning X friction factor $S_{fx}$ , m <sup>-1/3</sup> s	0.3 (grassland), 0.03 (pond)	HGS Introductory Manual
Manning Y friction factor $S_{fy}$ , m <sup>-1/3</sup> s	0.3 (grassland), 0.03 (pond)	HGS Introductory Manual
Rill storage height, m	0.05 (grassland), 0.01 (pond)	HGS Introductory Manual
Coupling length $l_{etch}$ , m	0.01	HGS Introductory Manual
Longitudinal dispersivity $a_L$ , m	5-15	Assessed by trial-and-error
Transverse dispersivity, $a_T$ m	1-3	Assigned $a_T=0.2 a_L$

<i>E. coli</i> die off rate in water, $k_{s,m,2}(20)$ , $d^{-1}$	0.056	Blaustein et. al (2013)
Parameter $Q_{10,m}$	1.415	Blaustein et. al (2013)
Evaporation depth, m	0.3	HGS Introductory Manual
Root depth, m	1.8	
Leaf area index (LAI)	2.08	HGS Introductory Manual
Transpiration fitting parameters: C1, C2, C3	0.1, 0.05, 2.0	HGS Introductory Manual
Wilting point pressure head, m	-150	HGS Introductory Manual
Field capacity pressure head, m	-3.8	HGS Introductory Manual
Evaporation limiting pressure heads	Min: -1.5, Max: -0.5	HGS Introductory Manual
Canopy storage parameter	0.	HGS Introductory Manual

240

241 *E. coli* fate and transport simulations were performed for 2022-2023. To progress the numerical convergence and reduce  
 242 simulation time, we use relative concentrations  $C_r = C/C_{max}$ , where  $C_{max} = 1.4 \cdot 10^{10}$  MPN·m<sup>-3</sup> is the maximum value of boundary  
 243 concentration at the soil surface. The value of the longitudinal dispersivity values for the porous media domain was chosen to  
 244 be 10 m, considering the scale problem (Neuman, 1990). There is no data concerning longitudinal dispersivity for the overland  
 245 flow domain. Therefore, we tested a few values of this parameter from 5 to 15 m. Longitudinal dispersivity equal to 12.5 m  
 246 produced a better agreement between simulated and observed concentrations. The transverse dispersivities were 1/5 of the  
 247 longitudinal ones for porous media and overland flow domains.

248 *E. coli* die-off/inactivation rates exhibit considerable variability depending on environmental conditions, e.g.,  
 249 temperature, moisture, pH, organic matter content, attachment to particles, solar radiation, predation, and matrix type such as  
 250 manure, soil, runoff, or pond water (Lim and Flint, 1989; Soupir, 2007; Ravva and Korn, 2007; Muirhead, and Littlejohn,  
 251 2009; Oliver et al., 2010; Tran et al., 2020). The *E. coli* die-off parameters in Table 1 and 2 were taken as average over the  
 252 parameters for datasets presented in published databases. The Q10 model parameters of *E. coli* survival in water were averages  
 253 over 16 survivals in wastewater datasets presented in the work of Blaustein et al (2013), and the Q10 model parameters of *E.*  
 254 *coli* survival in manure were averages over seven experimental datasets with bovine manure published by Martinez et al.  
 255 (2013). The *E. coli* temperature-dependent die-off in manure, soil, and water was simulated. The current version of HGS does  
 256 not allow the die-off rate in the surface flow domain to be prescribed as a function of temperature. Therefore, this parameter  
 257 (Tables 1 and 2) was re-calculated for each three-month-long season using mean temperature values and used piecewise by  
 258 restarting simulations for each time interval.

259 **3. Results and discussion**

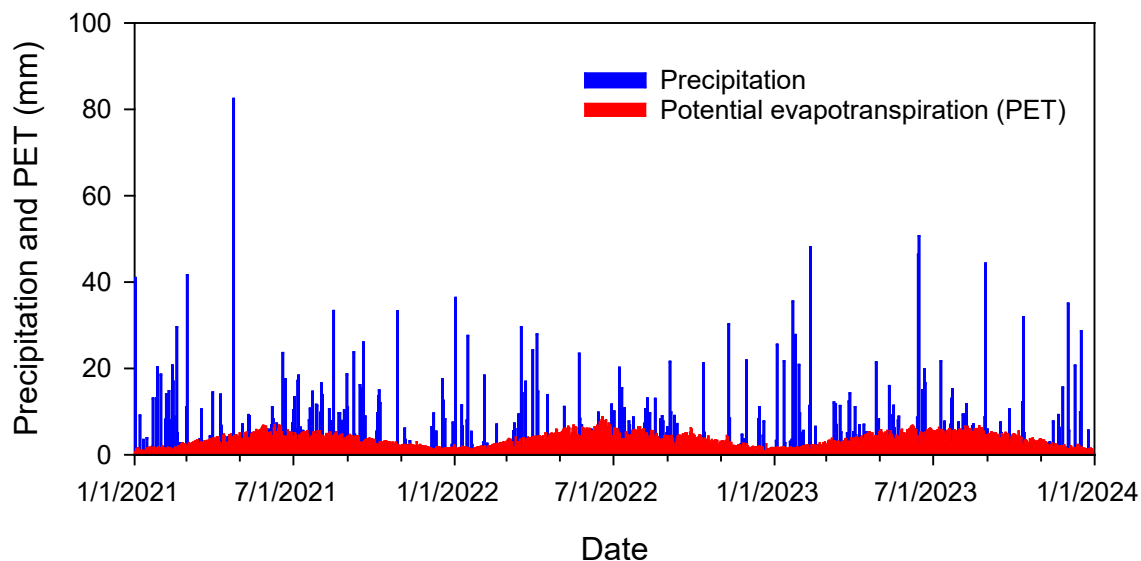
260 **3.1. *E. coli* boundary conditions and internal source terms**

261 All simulations were carried out using available weather data for a time interval from January 1, 2021, to December 31, 2023.

262 Annual precipitation was 1375, 998, and 1167 mm in 2021, 2022, and 2023, respectively. Figure 4 shows rainfall and calculated

263 potential evapotranspiration in the study area in 2021-2023.

264



265

266 **Figure 4. Precipitation and calculated potential evapotranspiration.**

267

268 The surface Cauchy-type boundary concentration at the grazing area (Figure 3a) was calculated using the equations presented

269 in Appendix A, as described above in section 2.3.3. We assume that 50 cattle (the maximum number of animals that appeared

270 in monitoring camera photos) were grazing in the watershed. The total grassland area of around 60000 m<sup>2</sup> was estimated based

271 on recent aerial imagery provided in Google Earth (version Pro 7.3). Nennich et al. (2005) estimated the average daily load of

272 manure of 38.6 and 66.3 kg·day<sup>-1</sup>·cow<sup>-1</sup> for dry and lactating cows, respectively. The ratio of urine to feces in dairy cows varies,

273 but on average, slightly less than one-third of manure is urine. Thus, we estimate average daily feces excretion as

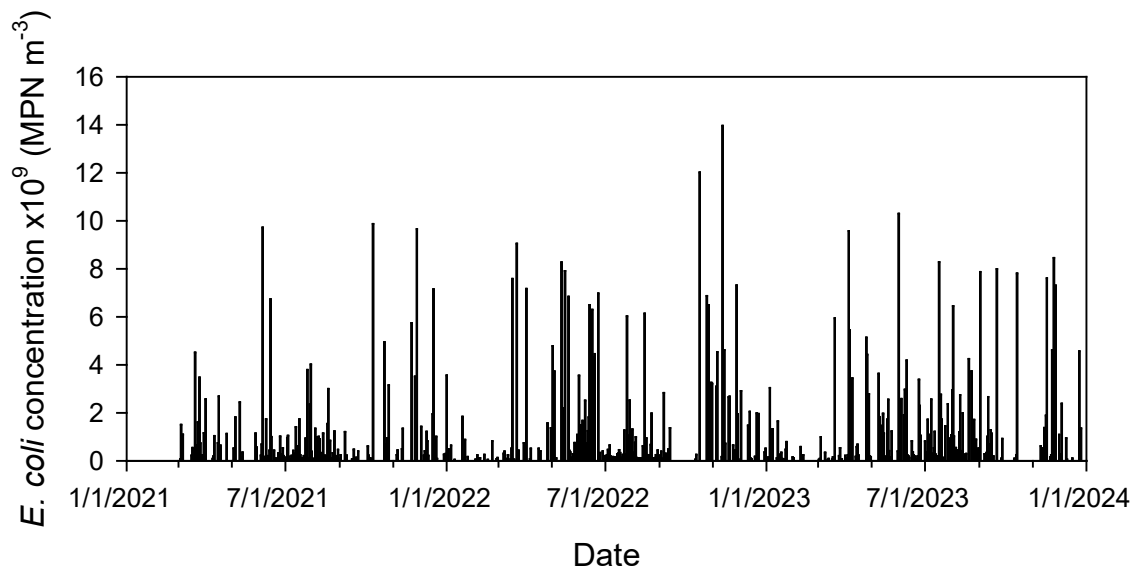
274  $0.5 \cdot (38.6 + 66.3) \cdot 0.667 = 35 \text{ kg} \cdot \text{day}^{-1} \cdot \text{cow}^{-1}$ . Monitoring shows that during the day, cows usually graze for at least 12 hours.

275 Therefore, we estimate solid manure load  $M_0 = \text{kg} \cdot \text{day}^{-1} \cdot \text{cow}^{-1} \cdot 12 \text{h} / 24 \text{h} \cdot 50 \text{ cows} / 60000 \text{ m}^2 = 0.0146 \text{ kg} \cdot \text{m}^{-2}$ . The initial

276 concentration of *E. coli* in fresh cowpats,  $m_{i0} = 7.38 \cdot 10^8 \text{ MPN} \cdot \text{kg}^{-1}$ , was calculated as an average in 16 samples collected in

277 2023. Other parameters in equations A3-A4 were  $\alpha_m = 23.375 \text{ h}^{-1}$ ,  $\beta_m = 1.732$ , and  $E_r = 1$  (Stoker et al., 2018). No cattle

278 were observed in the field from the beginning of December to the end of February. Figure 5 shows the calculated boundary  
279 concentrations.

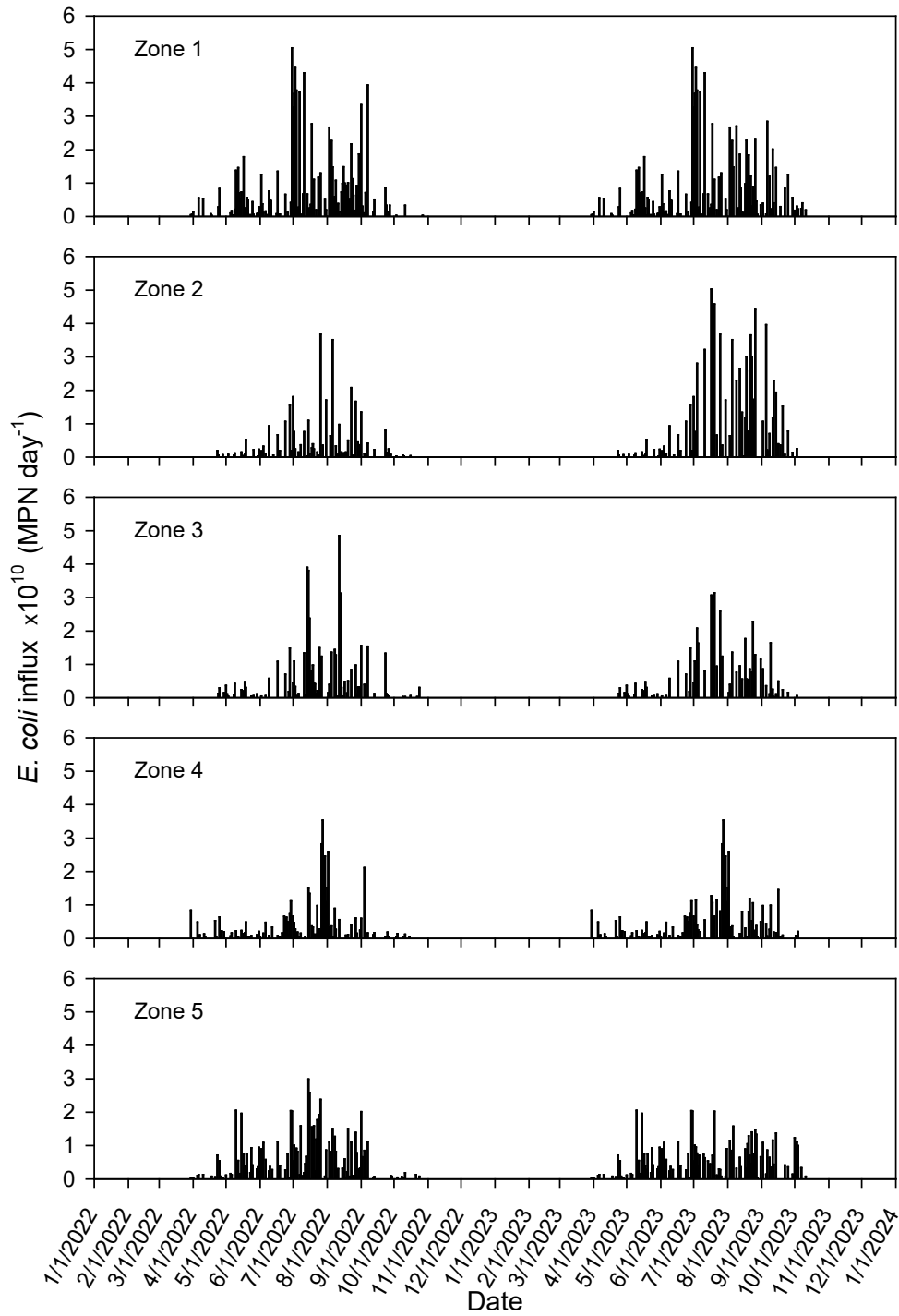


280

281 **Figure 5. Simulated temporal variation of *E. coli* surface boundary concentration at the grazing land.**

282

283 **The influx of source terms representing *E. coli* loading from direct cattle excretion into the pond was calculated as described**  
284 **in Section 2.4.3.** Validation of the visual assessment of trail camera imagery to derive Cex yielded strong correlations among  
285 the three observers (OBS1 v OBS2, n = 64, R<sup>2</sup> = 0.93; OBS1 v OBS3, n = 46, R<sup>2</sup> = 0.90; OBS2 v OBS3, n = 18, R<sup>2</sup> = 0.99). It  
286 was assumed that all bacteria were immediately released from manure in the pond. Accounting for the daily cow excretion (as  
287 explained above for the surface boundary concentration) and *E. coli* concentration in cowpats, we calculated the daily source  
288 rate for each pond zone (Figure 6) as a portion of the daily manure excretion. The rate for each node is one-tenth of the zone  
289 rate. Cattle use monitoring started in July 2022. Therefore, in simulations for the period January-June 2022, where there were  
290 no observations, the calculated rates for 2023 were used.



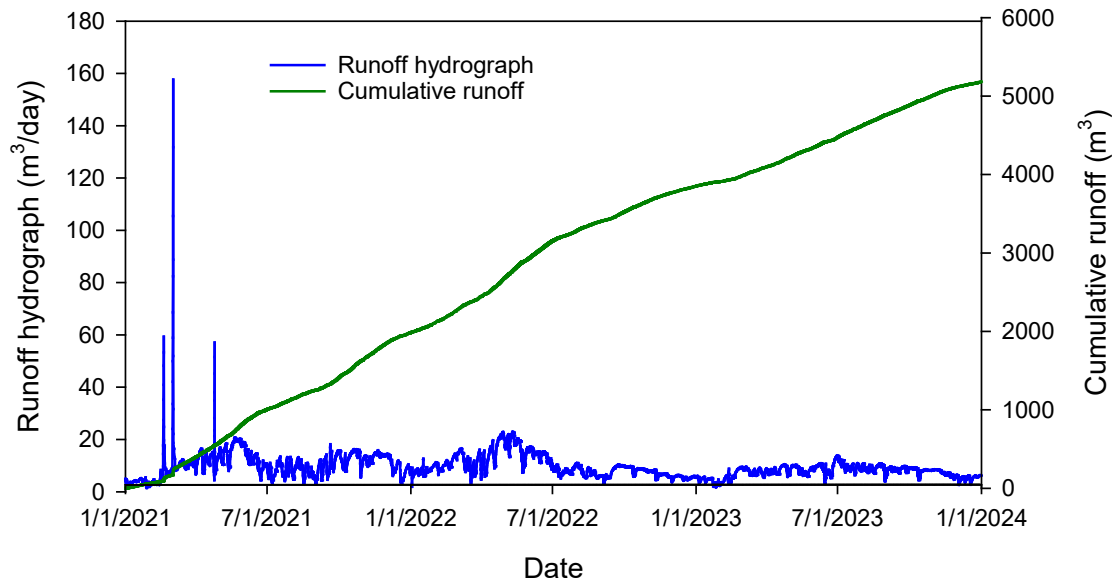
291  
 292 **Figure 6. Calculated *E. coli* inputs to the pond through cattle excretion for the five zones.**

294 **3.2. Flow simulation results**

295 Water flow simulations were carried out for 2021-2023. The simulated water level in the pond is controlled by a balance of  
 296 inflows (precipitation and overland runoff) and outflows (evaporation, infiltration through the pond bottom and dam). To  
 297 ensure realistic pond persistence during the multi-year simulation period, while preventing unrealistic complete drying while  
 298 avoiding excessive overflow, we fitted the hydraulic conductivity of the clay liner at the pond bottom to a value of 0.0002  
 299 m/day. Increasing this parameter above 0.0002 m/day resulted in excessive seepage losses, leading to a significant and  
 300 unrealistic decline in the simulated pond water level over the simulation period, which was inconsistent with observed or  
 301 expected pond behaviour in the study area.

302 The rest of the parameters are presented in Table 1. During periods with high precipitation, perched water was developed  
 303 above the clay layer (around 0.5 m below the land surface, not shown). Daniels et al. (1978) reported that soil horizons having  
 304 10% of platy plinthite will perch water.

305 Runoff is rarely observed in the area. The HGS model calculates fluid fluxes across the pond boundary. Water fluxes are  
 306 computed between active nodes (located on the pond boundary—dark blue dots in Figure 3a) and contributing nodes (located  
 307 just outside the pond boundary). The calculated surface water flux represents the simulated runoff to the pond (Figure 7).



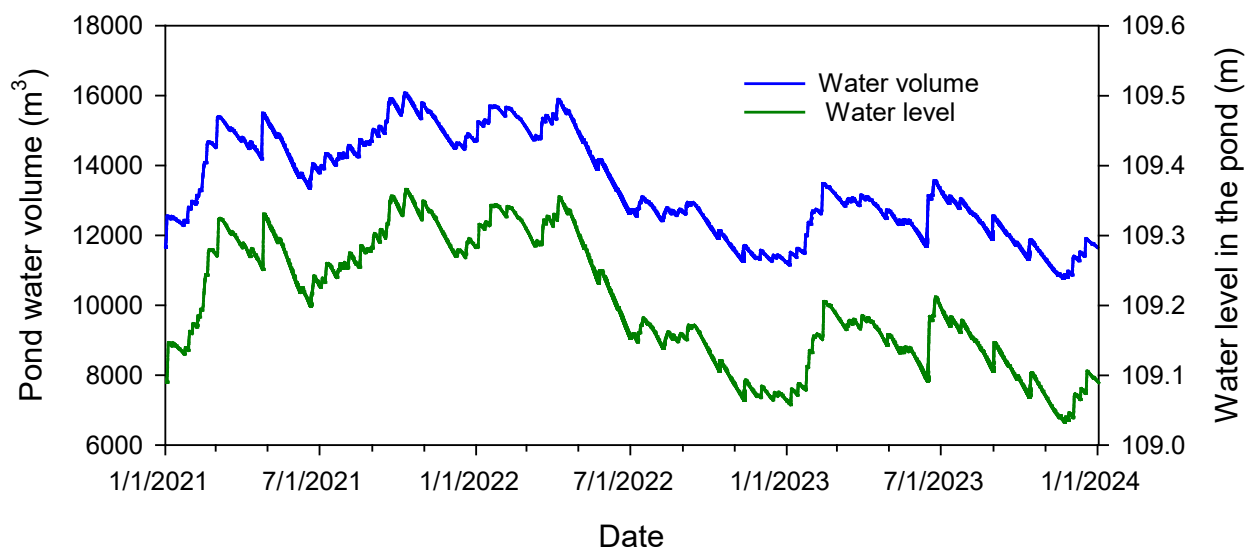
308

309 **Figure 7. Computed runoff to the pond.**

310 At the beginning of 2021, three significant flow events occurred after intensive 30, 50, and 82 mm rainfalls on February 18,  
 311 Mar 1-2, and April 24, respectively. During the rest of the time, the average computed surface flow rate to the pond is around

312 4.4 m<sup>3</sup>·day<sup>-1</sup>. The latter is a relatively small value given a 650 m-long pond perimeter. This small but persistent surface water  
313 inflow to the pond during dry periods (no precipitation), attributable to slow drainage of shallow subsurface lateral flow  
314 (interflow or return flow) from upslope areas that daylights and reaches the pond via surface pathways. This is distinct from  
315 precipitation-driven overland flow/surface runoff, which occurs only during or immediately following rainfall events  
316 (Tarboton, 2003).

317 Simulated changes to pond water volume (m<sup>3</sup>) and water level (mamsl) were tracked over the study period (Figure 8). The  
318 simulated minimal and maximal water levels were 109.03 and 109.37 mamsl. A rise in water level by 0.34 m causes an increase  
319 in water volume from 10770 to 16075 m<sup>3</sup>.



320

321 **Figure 8. Simulated temporal variation of water volume and level in the pond (above mean sea level).**

322

323

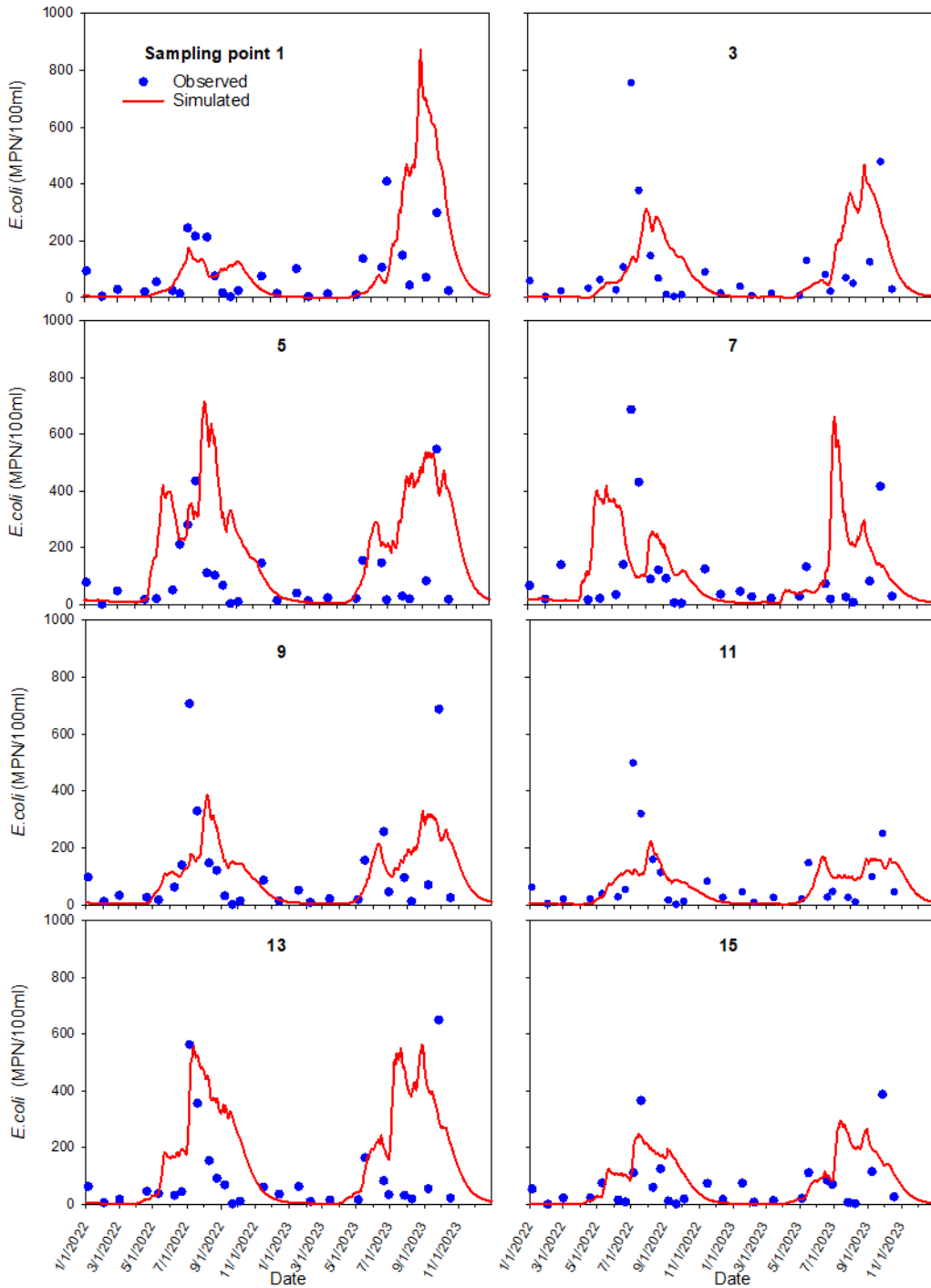
### 324 3.3. Bacteria fate and transport simulations

#### 325 3.3.1. Results for individual locations

326

327 Observed and simulated *E. coli* concentrations in the interior and nearshore pond sampling locations were compared for each  
328 sample location (Figures 9 and 10). The non-calibrated model tolerably mimicked *E. coli* concentration patterns and times of  
329 peak events in many of the pond's sampling locations. Concentrations increased during summer and decreased during winter  
330 months.

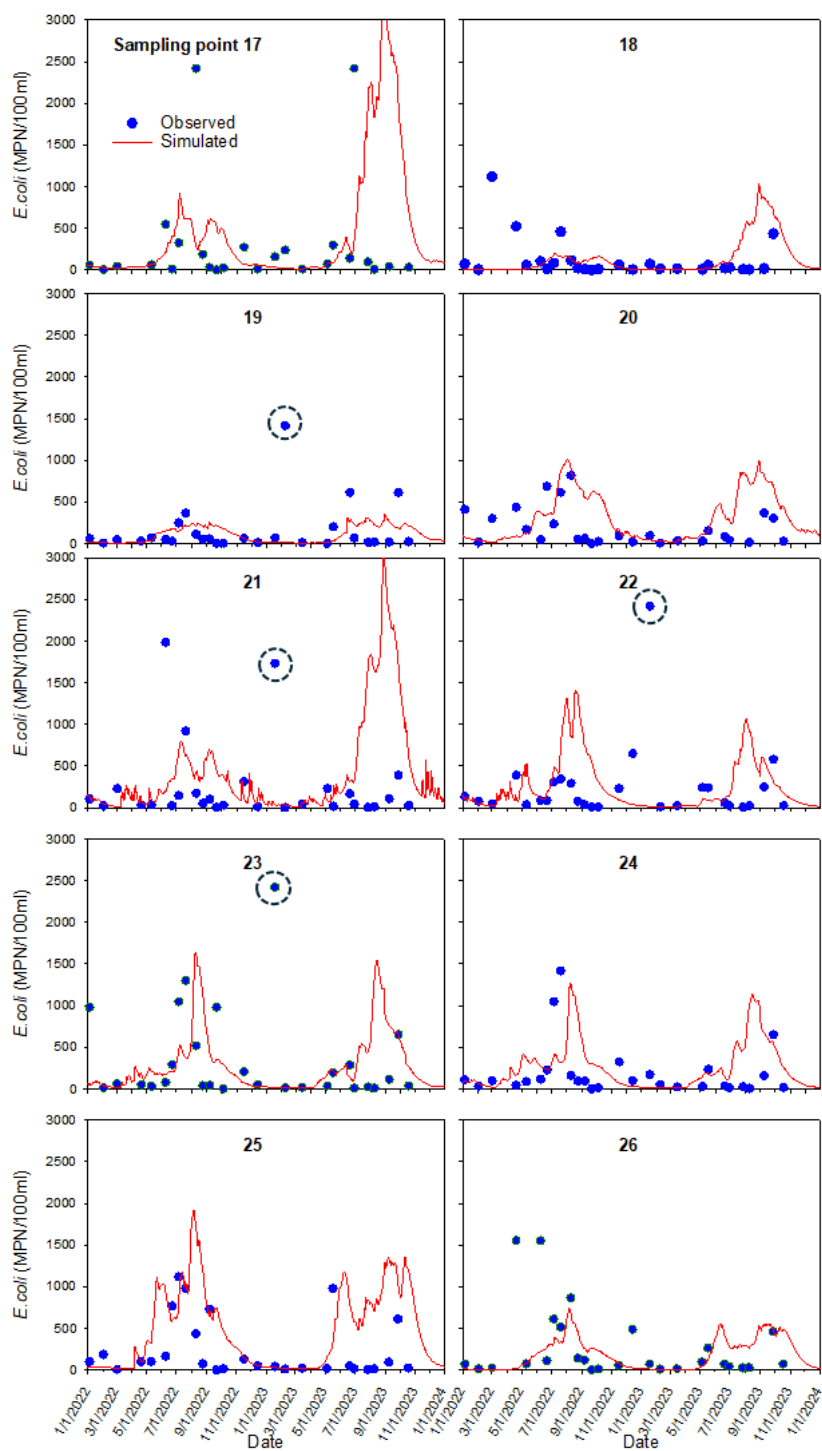
331 For the internal sampling locations 1 to 15, correlation coefficients between the monitored and simulated *E. coli*  
332 concentrations varied between 0.24 and 0.44. An exception was location 7, where the correlation coefficient was -0.01. For  
333 the near-shore sampling locations 17 to 26, the correlation coefficient varied between -0.15 and 0.32.  
334



335

336 **Figure 9. Observed (blue dots) and simulated (red line) *E. coli* concentrations at interior sampling locations 1-15.**

337



339 **Figure 10. Observed (blue dots) and simulated (red line) *E. coli* concentrations at nearshore sampling locations 17-26. Dashed circles**  
340 **indicate winter increases in concentrations on January 18, 2023.**

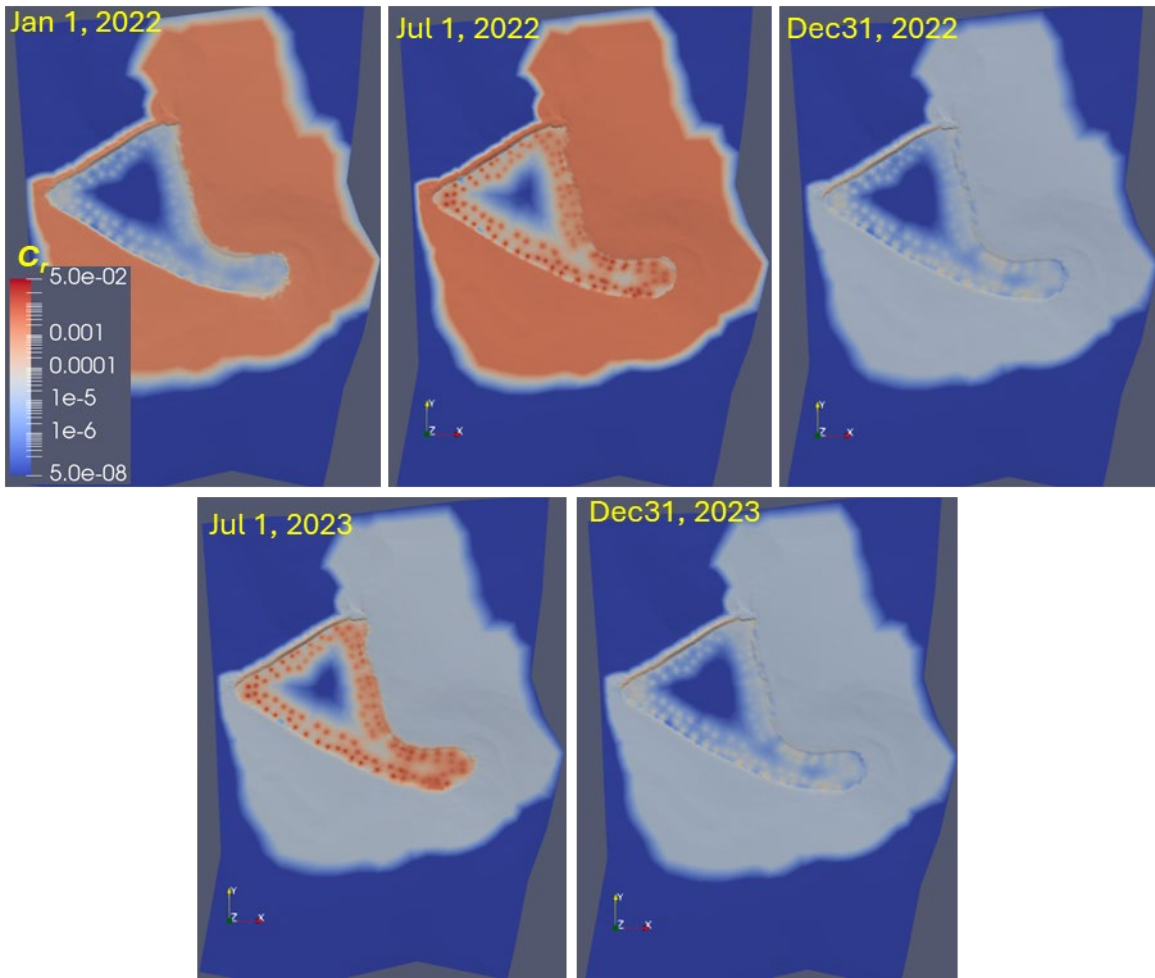
341

342 The observed differences between simulated and measured concentrations in individual sampling locations might  
343 originate from the model setup and computational features. The simulated concentration peaks strongly depended on the  
344 proximity of the sampling points to the internal source locations, which were constant in time. Cattle frequently moved across  
345 the pond in different directions, which affected the concentration distribution. Most assigned locations for the pond's internal  
346 source were 10-20 m from the nearest sampling point.

347 The reproduction of mixing in the pond might be locally unsatisfactory. Figure 11 shows the simulated relative *E.*  
348 *coli* concentration distribution at the surface for different dates. **Concentration in the source locations, simulating cattle**  
349 **excretion in the pond (Figure 3a),** rises during summer and dissipates in the winter. Simulations show a low *E. coli*  
350 concentration zone in the middle of the pond during the entire simulation period. For example, the model underpredicts peak  
351 concentration at sampling location 15 (Figure 9) in summer 2022 and autumn 2023. This indicates that mixing in the pond was  
352 stronger than the dispersion mechanism suggests. Lateral transport is often dependent on persistent wind-forced circulation.  
353 Henderson et al. (2024) describe wind-forced processes responsible for ponds' vertical mixing or lateral transport. Additional  
354 mixing resulting from induced eddies may cause more rapid cross-pond mixing and potentially affect pond ecology and  
355 biogeochemistry. At sampling location 23, the increase in concentration could be due to the occasional resuspension of bacteria  
356 from the bottom sediments during sampling.

357

358



359

360

361 **Figure 11.** Simulated spatiotemporal distribution of the relative *E. coli* concentration at the surface.  $C_r=C/C_{\max}$ ,  $C_{\max}=1.4 \cdot 10^{10}$

362  $\text{MPN}\cdot\text{m}^{-3}$ , the legend is on a log scale.

363

364

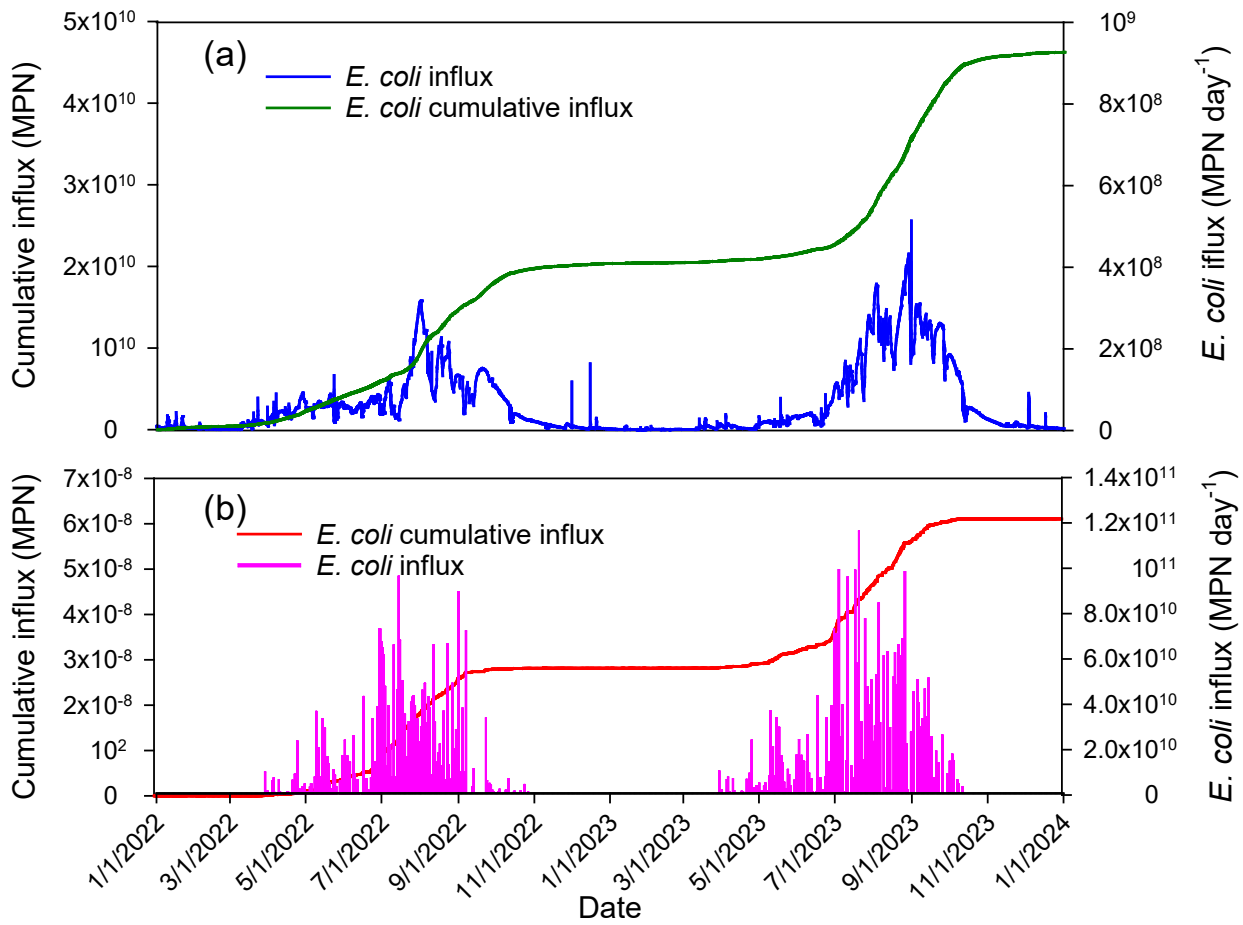
365

366 More insight could be expected from considering the specifics of *E. coli* survival in waters rich in organic matter and  
367 nutrients (Cho et al., 2021). Blaustein et al (2013) analyzed the database on *E. coli* survival in various surface waters. They  
368 found that the logarithm of *E. coli* remained approximately constant or even grew for some lag period time after the inactivation  
369 experiments in wastewaters with high content of organic matter and nutrients. After the lag period. The dependence of log C  
370 on time changed to a linear decrease. No model has been proposed to estimate the duration of the lag period in wastewater so  
371 far.

372 A sudden rise in *E. coli* concentration was observed on January 18, 2023, at sampling locations 19, 21, 22, and 23  
373 (Figure 9, dashed circles). The model does not reproduce this increase. The monitoring camera photos show flocks of birds in  
374 the pond near the first three locations 1 to 2 days before the sampling date. At the same time, the model's internal sources on  
375 that day were equal to zero since there were no cattle in the pond. We hypothesized that excretion by birds was a reason for  
376 elevated *E. coli* concentrations. During the fall and winter, Georgia's inland freshwaters become populated with waterfowl  
377 such as ducks, Canada geese, and migratory birds (Balkcom et al., 2025). One duck generates on average  $3.8 \cdot 10^{10}$  *E. coli* CFU  
378 per day (Moriarty et al., 2011), which is similar to the daily *E. coli* output from one cow ( $4 \cdot 10^{10}$  MPN (g wet feces)<sup>-1</sup> day<sup>-1</sup>  
379 in this work). It appears that the contribution of waterfowl can be very substantial in comparison with cattle contributions (see  
380 Figure 5). To our knowledge, the fraction of waterfowl excreta that enters water has not been reported in the literature. Overall,  
381 we concur with Vasquez et al. (2021) who emphasized the need to collect more data on the fecal contamination inputs of the  
382 ponds.

### 383 3.4. Results for the pond as a whole

384 The HGS computed temporal *E. coli* fluxes entering the pond with surface water. The influxes of *E. coli* to the pond were  
385 visualized along with their calculated cumulative numbers over time for both sources of runoff (Figure 12a) and direct  
386 excretion of feces (Figure 12b). At the end of simulations, the number of bacteria entering the pond by manure excretion was  
387 around 130 times greater than by surface runoff. Simulations show that water flowed mainly from the pond into the subsoil,  
388 so that *E. coli* concentrations in the subsoil did not affect the water quality in the pond. .



389  
 390 **Figure 12. Simulated *E. coli* fluxes to the pond: (a) with runoff; (b) excreted into the pond.**  
 391

392

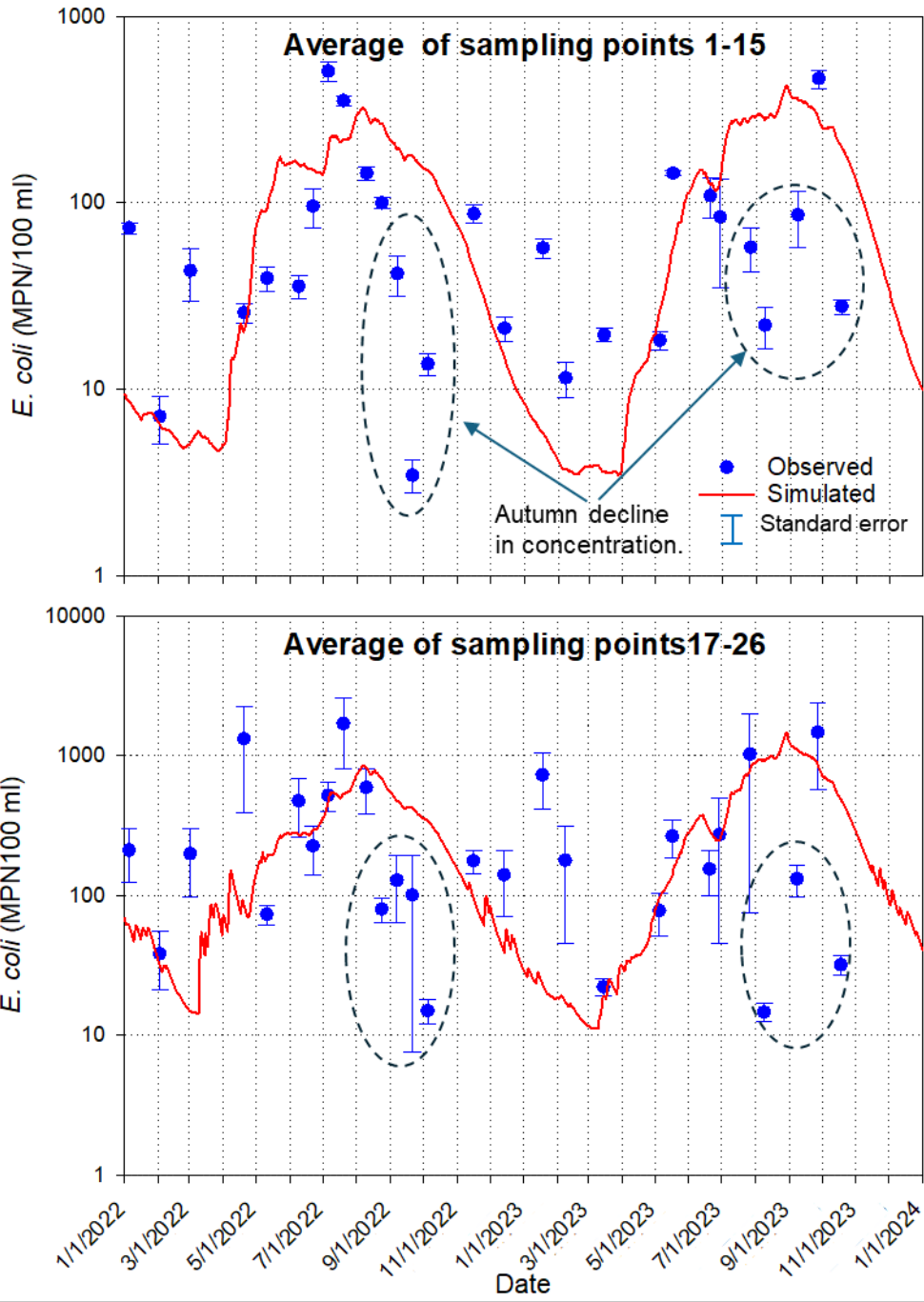
393

394 Simulated and observed concentrations of *E. coli* were each averaged over the interior and nearshore sampling  
395 locations (Figure 13). Averaged values of concentrations at the nearshore locations (17-26) were approximately three times  
396 higher than the average of concentrations sampled at interior locations (1-15). Elevated nearshore concentrations may be  
397 explained by flushing bacteria to the pond during runoff and direct excretion by bathing cattle, which, according to monitoring,  
398 spent most of their time grouped close to the shore.

399 The summary data in Figure 13 show that the model describes seasonal average concentration patterns relatively well.  
400 However, observed concentrations significantly declined during autumn 2022 and 2023 compared to the model simulation.  
401 Clear, shallow water can cause deeper penetration of solar radiation. De Brauwere et al. (2014) indicate that the inactivation  
402 of bacteria is caused by UV irradiation. To account for the latter, some models add a term to the overall decay parameter due  
403 to sunlight (McCorquodale et al., 2004) or use a decay term depending on the intensity of the solar radiation (Kashefipour et  
404 al., 2006). The decrease in the nutrients in water in the fall can also be the reason for the reduction of *E. coli* concentration.

405 The descriptive statistics of measured and simulated average concentrations were close when computed over the  
406 observation period. The minimum and maximum averages across the pond concentrations were 3.56 and 525.1 for observed  
407 and 4.08 and 479.4 MPN (100 mL) for simulated data, respectively. The mean logarithms of average concentrations were  
408  $1.70 \pm 0.47$  and  $1.99 \pm 0.67$  for the measured and simulated data, respectively. The correlation coefficient between measured  
409 and simulated logarithms of average concentrations was 0.483. This value was significant at a 0.01 significance level and  
410 indicated a moderate correlation.

411



412  
 413 **Figure 13. Average *E. coli* concentrations in the pond's interior (1-15) and nearshore (17-26) sampling locations. Dashed circles**  
 414 **indicate an autumn decline in concentrations.**

415

#### 416 4. Discussion

417 Applying mechanistic fate and transport models relies on model parameter values typically obtained via model calibration.  
418 Several factors make the site-specific calibration of microbial fate and transport parameters difficult and sometimes unfeasible.  
419 The spatiotemporal variability of microbial concentrations in ponds is very high (Havelaar et al., 2017; Stocker et al., 2022),  
420 indicating the need to collect large numbers of samples. The collection and analysis of those samples appear to be unfeasible.  
421 That precludes establishing a proper monitoring program for efficient model calibration. The high spatiotemporal variability  
422 emphasized the scale mismatch between the water sample size and the water volume, and this sample is used to characterize a  
423 much larger water volume used for mass balance computation in the hydrological models.

424 Flow sub-model parameters have satisfactorily estimated more easily obtainable properties, such as clay or sand content  
425 and bulk density (Schaap et al., 2001). Analogous predictive relationships have not been developed, partially because the  
426 potential predictors of microorganism survival or release rate have been shown to be dependent on environmental variables  
427 that were themselves variable in space and time.

428 Compendia of microorganism release and survival parameters (Park et al., 2016) show that the parameter values  
429 encompass wide numerical ranges and that it is challenging to attribute fate and transport parameter values to specific  
430 environmental conditions or management practices. These factors so far substantially limit the applicability of microbial fate  
431 and transport modeling. On the other hand, such modeling is in demand due to the need for projections of microbial water  
432 quality changes due to environmental changes, adaptation practices, site-specific trade-offs between different water quality  
433 aspects, multiple ownership and management along or around irrigation water sources, etc.

434 In this situation, a relatively important question is: What accuracy can be expected in fate and transport predictions made  
435 with average or typical fate and transport parameter values? In other words, given the high spatial variability of microbial  
436 concentrations, how significant are the differences between observed and simulated concentrations with average parameter  
437 concentrations? The answers to those questions are surprisingly scarce, as the published modeling reports focus on calibration  
438 results. These questions have not been researched for agricultural ponds. Results of this work show that if the animal behavior  
439 patterns are known, the seasonal trends and magnitudes of pond water microbial pollution can be estimated. Quantifying such  
440 patterns for cattle ponds has not been done so far. However, it presents a promising avenue for research.

441 We realize that the system parameters we have studied are subject to multiple sources of uncertainty. Quantifying this  
442 uncertainty and running ensemble simulations with parameters treated as random values presents an interesting avenue for  
443 future research. Results of this work, obtained with mean parameter values from various sources, indicate that determining the  
444 statistical properties of the bacteria sources can be a first feasible step in that direction.

445 The present model does not incorporate explicit simulation of soil and manure erosion, suspended sediment transport,  
446 settling, or resuspension processes. This omission may underestimate bacterial concentrations in receiving waters during high-  
447 flow events, when sediment resuspension, potentially exacerbated by cattle trampling or other disturbances can act as an  
448 important secondary source of fecal indicator bacteria. Numerous studies have highlighted the significance of sediment-

449 associated bacterial transport and resuspension in agricultural watersheds (e.g., Jamieson et al., 2005; Pandey et al., 2012;  
450 Bradshaw et al., 2021). Future model extensions could benefit from coupling a sediment transport sub-module to more  
451 comprehensively capture these interactions.

452 The current implementation does not include site-specific calibration or formal sensitivity analysis of key parameters (e.g.,  
453 die-off rates, sorption coefficients as listed in Tables 1 and 2). While these steps would provide valuable insights into parameter  
454 influence and model behavior, and are recommended for future applications, the present work prioritizes proof-of-concept  
455 integration and qualitative assessment over quantitative optimization. Similarly, the model currently incorporates a single  
456 dominant removal process (first-order die-off/inactivation) to maintain simplicity during initial coupling; additional  
457 mechanisms (e.g., settling, resuspension, or biotic interactions) were not included but represent promising extensions. Such  
458 enhancements could better elucidate ecosystem functioning and inform management strategies to enhance bacterial removal  
459 in pond systems, as supported by prior modeling efforts in watershed-scale microbial fate and transport (e.g., Ferguson et al.,  
460 2010; Bradford et al., 2013; Cho et al., 2016).

461 This study contributes to the current state-of-the-art in several ways. First, it applies a fully mechanistic three-dimensional  
462 surface–subsurface hydrological model to simulate microbial fate and transport in and around a cattle pond. Unlike many  
463 previous studies that rely on simplified or lumped representations of microbial transport, the present approach explicitly  
464 resolves hydrological processes controlling bacterial transport through surface runoff and subsurface flow pathways at the  
465 watershed scale. Second, the model explicitly accounts for direct microbial loading caused by cattle entering the pond and  
466 depositing manure in the water. The magnitude of this source term was estimated from the observed presence of cattle in the  
467 pond using time-lapse imagery obtained from multiple trail cameras. To our knowledge, such direct observational  
468 quantification of livestock behavior has rarely been incorporated into mechanistic watershed-scale microbial transport models.  
469 Third, the study evaluates the ability of a mechanistic model to reproduce observed *E. coli* dynamics with minimal calibration  
470 using primarily literature-based parameter values. This approach addresses a common limitation in agricultural water quality  
471 studies, where extensive datasets required for model calibration are rarely available. Finally, the modeling framework provides  
472 quantitative insight into the relative importance of different contamination pathways, including surface runoff from manure  
473 deposited on pasture and direct microbial loading by cattle entering the pond. The results demonstrate that direct excretion by  
474 cattle in the pond can dominate microbial inputs under certain management conditions. Overall, this work demonstrates how  
475 mechanistic watershed-scale modeling combined with observational data on livestock behavior can be used to improve  
476 understanding and prediction of microbial contamination in agricultural ponds.

477  
478  
479

## 480 5. Conclusions

481 This study developed the first mechanistic numerical model for bacteria transport from grazing land around a cattle pond. The  
482 model was based on the HGS software, simulating fully coupled surface-subsurface flow and transport. The model was tested  
483 to simulate *E. coli* fate and transport in a small pastureland watershed in Georgia, USA, using observations from 2021-2023.  
484 The primary goal was to simulate the temporal and spatial distribution of *E. coli* concentration in the pond. All parameters for  
485 this simulation were taken from the literature or estimated from published data. The exception was the rate of *E. coli* input to  
486 the pond from the direct excretion of feces from animals, since such data were not found in the literature. The non-calibrated  
487 model could mimic *E. coli* temporal concentration patterns and peak times reasonably well in most of the pond's sampling  
488 locations. There were seasonal differences in correspondence between simulated and measured *E. coli* time series, and the  
489 magnitude of concentration peaks was poorly predicted in some sampling locations. Predictions of the average across-pond  
490 concentrations were expected to be moderately accurate. Quantification of microbial inputs for cattle ponds has not been done  
491 so far. Still, it presents a promising avenue to estimate the microbial water quality in cow ponds using the data accumulated in  
492 past research.

493

494

## 495 Author contributions

496 AY: methodology, investigation, formal analysis, software, writing - original draft; AC: supervision, methodology,  
497 investigation, data acquisition, resources, formal analysis, writing – review and editing; JW: data acquisition, resources; OP:  
498 resources, writing – review and editing, RH: supervision, software; YP: conceptualization, project administration, funding  
499 acquisition.

## 500 Declaration of competing interest

501 The authors declare that they have no known competing financial interests or personal relationships that could have appeared  
502 to influence the work reported in this paper.

## 503 Acknowledgements

504 This research was supported by the USDA-ARS projects (6048-13000-028-000D "Shifting the Balance of Water Resources  
505 and Interacting Agroecosystem Services toward Sustainable Outcomes in Watersheds of the Southern Coastal Plain," non-  
506 assistance cooperative agreements 58-8042-3-030 "Modeling Fate and Transport of Indicator and Pathogenic Organisms to  
507 Assess Microbial Water Quality of Irrigation Water Sources, "and 58-8042-0-064 "Monitoring and Modeling Microbial  
508 Quality of Irrigation Water"

509 **Data availability**

510 Data will be made available on request.

511

512

513 **Appendix A: Equations to calculate *E. coli* concentration released from cowpats at the soil surface (3<sup>rd</sup>-kind boundary**  
514 **condition concentration).**

515 For day  $t$ , the content of microorganism in the applied manure is calculated by (Martinez et al., 2013):

516

$$517 \quad m_i(t) = m_i(t - 1)e^{-k_{s,m}} \quad (A1)$$

519

518 Where  $k_{s,m}$  is the rate coefficient which is the function of temperature  $T$  at time  $t$ , ( $d^{-1}$ )

520

$$521 \quad k_{s,m} = \begin{cases} k_{s,m,1}, & t \leq t_{s,m,1} \\ k_{s,m,2}(T), & t > t_{s,m,1} \end{cases} \quad (A2)$$

522

523  $t_{s,m,1}$  is the duration of the first stage,  $d$ ,  $T$  is the average daily temperature, °C, and  $k_{s,m,1}$  and  $k_{s,m,2}(T)$  the survival rates at the  
524 first and second survival stages are respectively.

525 The bacterial population may grow, remain stable, or die off during the first survival stage, and decrease during the second  
526 stage of survival. On the second stage, the values of  $k_{s,m,2}(T)$  can be described with the Q10 model (Martinez et al., 2013).

527

$$528 \quad k_{s,m,2}(T) = k_{s,m,2}(20)Q_{10,m}^{\frac{T-20}{10}} \quad (A3)$$

529

530 where  $k_{s,m,2}(20)$  is the survival rate at 20 °C,  $Q_{10,m}$  reflects the sensitivity of  $k_{s,m,2}$  to a temperature that is equal to the change  
531 in survival rate occurring as temperature changes by 10 °C.

532 The concentration of released microorganism  $C_m$  is calculated according to Bradford and Schijven (2002) as

$$533 \quad C_{man}(t) = \frac{dM_{man}}{Rdt} = \frac{M_0\alpha_m}{R} (1 + \alpha_m\beta_m t)^{-(1+1/\beta_m)} \quad (A4)$$

534

$$535 \quad C_m(t) = m_i E_r C_{man}(t) \quad (A5)$$

536

537 Where  $M_{man}$  is the cumulative cowpat mass released into the aqueous phase (g),  $R$  is rain intensity, cm/h,  $\alpha_m$  ( $h^{-1}$ ) and  $\beta_m$  are  
538 fitting parameters defining the shape of the release curve, and  $M_0$  is the initial mass of cowpats ( $g/cm^2$ ),  $C_{man}$  is the aqueous

539 manure concentration ( $\text{g cm}^{-3}$ ),  $m_i$  is content of microorganism in the cowpats ( $\text{CFU g}^{-1}$ ),  $E_r$  is microorganism release  
540 efficiency.  
541

542 **References**

- 543 Balkcom, G., Touchstone, T., Kammermeyer, K., Vansant, V., Martin, C., Van Brackle, M., Steele, G., & Bowers, J.:  
544 Waterfowl management in Georgia. Georgia Department of Natural resources. Available at  
545 [https://georgiawildlife.com/sites/default/files/wrd/pdf/management/Waterfowl\\_Management\\_in\\_Georgia.pdf](https://georgiawildlife.com/sites/default/files/wrd/pdf/management/Waterfowl_Management_in_Georgia.pdf)  
546 [georgiawildlife.com](https://georgiawildlife.com). Last assessed on March 07, 2026.
- 547 Blaustein, R. A., Pachepsky, Y., Hill, R. L., Shelton, D. R., & Whelan, G.: Escherichia coli survival in waters: temperature  
548 dependence, Water research, 47(2), 569-578, <https://doi.org/10.1016/j.watres.2012.10.027>, 2013.
- 549 Blume, L.J., Perkins, H.F. and Hubbard, R.K.: Subsurface water movement in an upland coastal plain soil as influenced by  
550 plinthite, Soil Sci. Soc. of America J., 51(3), 774-779, <https://doi.org/10.2136/sssaj1987.03615995005100030036x>,  
551 1987.
- 552 Bosch, D. D., Sheridan, J. M., Lowrance, R. R., Hubbard, R. K., Strickland, T. C., Feyereisen, G. W., & Sullivan, D. G.: Little  
553 river experimental watershed database, Water Resources Research, 43(9), <https://doi.org/10.1029/2006WR005844>,  
554 2007.
- 555 Bradford, S.A., and J. Schijven.: Release of Cryptosporidium and Giardia from dairy calf manure: Impact of solution salinity,  
556 Environ. Sci. Technol. 36, 3916–3923, <https://doi.org/10.2134/jeq2004.1499>, 2002.
- 557 Bradford, S.A., Morales, V.L., Zhang, W., Harvey, R.W., Packman, A.I., Mohanram, A., and Welty, C.: Transport and fate of  
558 microbial pathogens in agricultural settings, Critical Reviews in Environmental Science and Technology 43, 775–  
559 893, <https://doi.org/10.1080/10643389.2012.710449>, 2013.
- 560 Bradshaw, J. K., Snyder, B. J., Oladeinde, A., Spidle, D., & Berrang, M. E.: Sediment and fecal indicator bacteria loading in  
561 a mixed land use watershed: Contributions from suspended sediment and bedload transport, Journal of Environmental  
562 Quality, 50(3), 598–611. <https://doi.org/10.1002/jeq2.20166>, 2021.
- 563 Cho, K.H., Pachepsky, Y.A., Kim, M., Pyo, J.C., Park, M.H., Kim, Y.M., Kim, J.W., Kim, J.H.: Modeling seasonal variability  
564 of fecal coliform in natural surface waters using the modified SWAT, J. Hydrol. 535, 377–385,  
565 <https://doi.org/10.1016/j.jhydrol.2016.01.084>, 2016.
- 566 Cho, K., Wolny, J., Kase, J. A., Unno, T., & Pachepsky, Y.: Interactions of E. coli with algae and aquatic vegetation in natural  
567 waters, Water research, 209, 117952., <https://doi.org/10.1016/j.watres.2021.117952>, 2021.
- 568 Curre, F., Therrien, R. and Schilling, O.S.: Explicit simulation of reactive microbial transport with a dual-permeability, two-  
569 site kinetic deposition formulation using the integrated surface-subsurface hydrological model HydroGeoSphere.  
570 Hydrology and Earth System Sciences, 29(20), 5383-5403, <https://doi.org/10.5194/hess-29-5383-2025>, 2025.
- 571 Daniels, R.B., Perkins, H.F., Hajek, B.F. and Gamble, E.E.: Morphology of discontinuous phase plinthite and criteria for its  
572 field identification in the Southeastern United States, Soil Science Society of America Journal, 42(6), 944-949,  
573 <https://doi.org/10.2136/sssaj1978.03615995004200060024x>, 1978.

574 Danielescu, S.: Development and Application of ETCalc, a Unique Online Tool for Estimation of Daily Evapotranspiration,  
575 Atmosphere-Ocean, 61(3), 135–147, <https://doi.org/10.1080/07055900.2022.2154191>, 2022.

576 David, M. M., and Haggard, B. E.: Development of regression-based models to predict fecal bacteria numbers at select sites  
577 within the Illinois River watershed, Arkansas and Oklahoma, USA, Water, Air, and Soil Pollution 215, 525–547,  
578 <https://doi.org/10.1007/s11270-010-0497-7>, 2011.

579 de Brauwere, A., Ouattara, N. K., & Servais, P.: Modeling Fecal Indicator Bacteria Concentrations in Natural Surface Waters:  
580 A Review, Critical Reviews in Environmental Science and Technology, 44(21), 2380–2453.  
581 <https://doi.org/10.1080/10643389.2013.829978>, 2014.

582 Ferguson, C., Husman, A.M. d. R., Altavilla, N., Deere, D., and Ashbolt, N.: Fate and transport of surface water pathogens in  
583 watersheds, Critical Reviews in Environmental Science and Technology 33, 299–361,  
584 <https://doi.org/10.1080/10643380390814497>, 2010.

585 Gao, G., Falconer, R.A. and Lin, B.:Modelling the fate and transport of faecal bacteria in estuarine and coastal waters, Marine  
586 pollution bulletin, 100(1), 162-168, <https://doi.org/10.1016/j.marpolbul.2015.09.011>, 2015.

587 Havelaar, A. H., Vazquez, K. M., Topalcengiz, Z., Muñoz-Carpena, R., & Danyluk, M. D.: Evaluating the US food safety  
588 modernization act produce safety rule standard for microbial quality of agricultural water for growing  
589 produce, Journal of food protection, 80(11), 1832-1841, <https://doi.org/10.4315/0362-028X.JFP-17-122>, 2017.

590 Henderson, S.M., Nielson, J.R., Mayne, S.R., Goldberg, C.S. and Manning, J.A.: Transport and mixing observed in a pond:  
591 Description of wind-forced transport processes and quantification of mixing rates, Limnology and Oceanography,  
592 69(9), 2180-2192, <https://doi.org/10.1002/lno.12658>, 2024.

593 Iqbal, M. S., Hofstra, N.: Modeling Escherichia coli fate and transport in the Kabul River Basin using SWAT, Human and  
594 Ecological Risk Assessment: An International Journal, 25(5), 1279–1297,  
595 <https://doi.org/10.1080/10807039.2018.1487276>, 2019.

596 Jamieson, R. C., Joy, D. M., Lee, H., Kostashuk, R., Gordon, R. J.: Resuspension of sediment-associated Escherichia coli in a  
597 natural stream, Journal of Environmental Quality, 34(2), 581–589. <https://doi.org/10.2134/jeq2005.0581>, 2005.

598 Kashefipour, S. M., Lin, B., and Falconer, R. A.:Dynamic modelling of bacterial concentrations in coastal waters: Effects of  
599 solar radiation on decay, In J. J. Guo, et al. (Eds.), Advances in hydraulics and water engineering, Vols. 1 and 2:  
600 Proceedings, World Scientific: Singapore, 993–998, [https://doi.org/10.1142/9789812776969\\_0183](https://doi.org/10.1142/9789812776969_0183), 2002.

601 Kondo T., Sakai N., Yazawa T., Shimizu Y.: Verifying the applicability of SWAT to simulate fecal contamination for  
602 watershed management of Selangor River, Malaysia, Science of The Total Environment, 774, 145075,  
603 <https://doi.org/10.1016/j.scitotenv.2021.145075>, 2021.

604 Lim, C.-H., Flint, K. P.: The effects of nutrients on the survival of Escherichia coli in lake water, Journal of Applied  
605 Bacteriology, 66(6), 559–569, <https://doi.org/10.1111/j.1365-2672.1989.tb04578.x>, 1989.

606 Mankin, K.R., Wang, L., Hutchinson, S.L. and Marchin, G.L.: Escherichia coli sorption to sand and silt loam soil, Transactions  
607 of the ASABE, 50(4), 1159-1165, DOI:10.13031/2013.23630, 2007.

608 Martinez, G., Pachepsky, Y. A., Shelton, D. R., Whelan, G., Zepp, R., Molina, M., & Panhorst, K.: Using the Q10 model to  
609 simulate E. coli survival in cowpats on grazing lands, *Environment International*, 54, 1-10,  
610 <https://doi.org/10.1016/j.envint.2012.12.013>, 2013.

611 McCorquodale, J. A., Georgiou, I., Canelos, S., and Englande, A. J.: Modeling coliforms in storm water plumes, *Journal of*  
612 *Environmental Engineering and Science* 3, 419–431, <https://doi.org/10.1139/s03-055>, 2004.

613 Moriarty, E. M., Karki, N., Mackenzie, M., Sinton, L. W., Wood, D. R., & Gilpin, B. J.: Faecal indicators and pathogens in  
614 selected New Zealand waterfowl, *New Zealand Journal of Marine and Freshwater Research*, 45(4), 679-688,  
615 <https://doi.org/10.1080/00288330.2011.578653>, 2011.

616 Muirhead, R.W., Littlejohn, R.P.: Die-off of *Escherichia coli* in intact and disrupted cowpats. *Soil Use and Management*, 25,  
617 389-394, <https://doi.org/10.1111/j.1475-2743.2009.00239.x>, 2009.

618 Nennich, T.D., Harrison, J.H., Vanwieringen, L.M., Meyer, D., Heinrichs, A.J., Weiss, W.P., St-Pierre, N.R., Kincaid, R.L.,  
619 Davidson, D.L. Block, E.: Prediction of manure and nutrient excretion from dairy cattle, *Journal of Dairy Science*,  
620 88(10), 3721-3733, [https://doi.org/10.3168/jds.S0022-0302\(05\)73058-7](https://doi.org/10.3168/jds.S0022-0302(05)73058-7), 2005.

621 Nueman S.P.: Universal scaling of hydraulic conductivities and dispersivities in geologic media, *Water Resources Research*,  
622 26 (8), 1749-1758, <https://doi.org/10.1029/WR026i008p01749>, 1990.

623 Oliver, D. M., Clegg, C. D., Heathwaite, A. L., & Haygarth, P. M.: Differential E. coli die-off patterns associated with  
624 agricultural matrices. *Environmental Science & Technology*, 40(18), 5720–5726. <https://doi.org/10.1021/es0603249>,  
625 2006

626 Pandey, P. K., Soupir, M. L., & Rehmann, C. R. (2012). A model for predicting resuspension of *Escherichia coli* from  
627 streambed sediments, *Water Research*, 46(1), 115–126. <https://doi.org/10.1016/j.watres.2011.10.019>

628 Park, Y., Pachepsky, Y., Shelton, D., Jeong, J., & Whelan, G.: Survival of manure-borne *Escherichia coli* and fecal coliforms  
629 in soil: temperature dependence as affected by site-specific factors, *Journal of Environmental Quality*, 45(3), 949-  
630 957, <https://doi.org/10.2134/jeq2015.08.0427>, 2016.

631 Ravva S.V, Korn A.: Extractable organic components and nutrients in wastewater from dairy lagoons influence the growth  
632 and survival of *Escherichia coli* O157:H7, *Applied and Environmental Microbiology*, 73(7):2191-21988, doi:  
633 10.1128/AEM.02213-06, 2007,

634 Schaap, M. G., Leij, F. J., & Van Genuchten, M. T.: Rosetta: A computer program for estimating soil hydraulic parameters  
635 with hierarchical pedotransfer functions, *Journal of hydrology*, 251(3-4), 163-176, [https://doi.org/10.1016/S0022-1694\(01\)00466-8](https://doi.org/10.1016/S0022-1694(01)00466-8), 2001.

637 Soupir M.L.: Fate and transport of pathogen indicators from pasturelands. Ph.d Thesis. Virginia Polytechnic Institute, 297 pp.,  
638 2007.

639 Stocker, M., Yakirevich, A., Guber, A., Martinez, G., Blaustein, R., Whelan, G., Goodrich, D., Shelton, D. and Pachepsky, Y.:  
640 Functional evaluation of three manure-borne indicator bacteria release models with multi-year field experiment data.  
641 *Water, Air, & Soil Pollution*, 229, 181, <https://doi.org/10.1007/s11270-018-3807-0>, 2018.

642 Stocker, M.D, Pachepsky, Y.A., Hill, R.L.: Prediction of *E. coli* Concentrations in Agricultural Pond Waters: Application and  
643 Comparison of Machine Learning Algorithms, *Front. Artif. Intell.* 4, 768650, doi: 10.3389/frai.2021.768650, 2022.

644 Sowah, R. A., Bradshaw, K., Snyder, B., Spidle, D., & Molina, M.: Evaluation of the soil and water assessment tool (SWAT)  
645 for simulating *E. coli* concentrations at the watershed-scale, *Science of the Total Environment*, 746, 140669,  
646 <https://doi.org/10.1016/j.scitotenv.2020.140669>, 2020.

647 Renwick, W.H, Oh, O.: Small artificial ponds in the United States: impacts on sedimentation and carbon budget, *Proceedings*  
648 *of the 8th Federal Interagency Sedimentation Conference.*, 738–744, Advisory Committee on Water Information, US  
649 Geological Survey, US Department of the Interior, Reston,  
650 VA <https://water.usgs.gov/osw/ressed/references/Renwick-2006-8thFISC.pdf>, 2006.

651 Stocker, M.D., Pachepsky, Y.A. and Hill, R.L.: Prediction of *E. coli* concentrations in agricultural pond waters: application  
652 and comparison of machine learning algorithms, *Frontiers in Artificial Intelligence*, 4, 768650, 2022.

653 Tarboton, D. G.: *Rainfall-runoff processes*, 159pp, Utah State University, 2003. available at: <https://hydrology.usu.edu/rrp/>.  
654 (last assessed on March 07, 2026).

655 Therrien, R., Sudicky, E. A., & McLaren, R. G.: *HydroGeoSphere: A Three-Dimensional Numerical Model Describing Fully-*  
656 *Integrated Sub-Surface and Surface Flow and Solute Transport*. Groundwater Simulations Group, University of  
657 Waterloo, Waterloo, ON 1-369, 2010.

658 van der Meulen, E. S., Tertienko, A., Blauw, A. N., Sutton, N. B., van de Ven, F. H. M., Rijnaarts, H. H. M., & van Oel, P.  
659 R.. A review of prediction models for *E. coli* in urban surface waters, *Urban Water Journal*, 21(5), 539–548.  
660 <https://doi.org/10.1080/1573062X.2024.2313634>, 2024.

661 Van Genuchten, M.T., 1980. A closed-form equation for predicting the hydraulic conductivity of unsaturated soils, *Soil science*  
662 *society of America journal*, 44(5), pp.892-898, <https://doi.org/10.2136/sssaj1980.03615995004400050002x>, 1980.

663 Vazquez, K,M, Muñoz-Carpena R., Danyluk M,D,, Havelaar A,H.: Parsimonious mechanistic modeling of bacterial runoff  
664 into irrigation ponds to inform food safety management of agricultural water quality, *Appl Environ Microbiol* 87:  
665 e00596-21, <https://doi.org/10.1128/AEM.00596-21>.

666 Watson, T.W. *The geohydrology of Ben Hill, Irwin, Tift, Turner and Worth counties, Georgia*, Hydrologic Atlas 2, Atlanta,  
667 1976.

668 Wolska, L., Kowalewski, M., Potrykus, M., Redko, V. and Rybak, B.: Difficulties in the modeling of *E. coli* spreading from  
669 various sources in a coastal marine area, *Molecules*, 27(14), p.4353, <https://doi.org/10.3390/molecules27144353>,  
670 2022.

671 Yao, F., Band, L. E., Cheng, F. Y., Rosentreter, J., Yang, K., & Wang, C.: A new high-resolution global lake area dataset for  
672 constraining biogeochemical fluxes from inland water bodies, *AGU Fall Meeting Abstracts*, 2024(1177), H53H-1177,  
673 2024.